



Since 1959

Atomically precise clusters for applications

T. Pradeep

Institute Professor, IIT Madras

<https://pradeepresearch.org/>

pradeep@iitm.ac.in

Professor-in-charge

Co-founder

InnoNano Research Pvt. Ltd.

InnoDI Water Technologies Pvt. Ltd.

VayuJAL Technologies Pvt. Ltd.

Aqueasy Innovations Pvt. Ltd.

Hydromaterials Pvt. Ltd.

EyeNetAqua Pvt. Ltd.

Deepspectrum Analytics Pvt. Ltd.



Associate Editor

ACS
Sustainable
Chemistry & Engineering

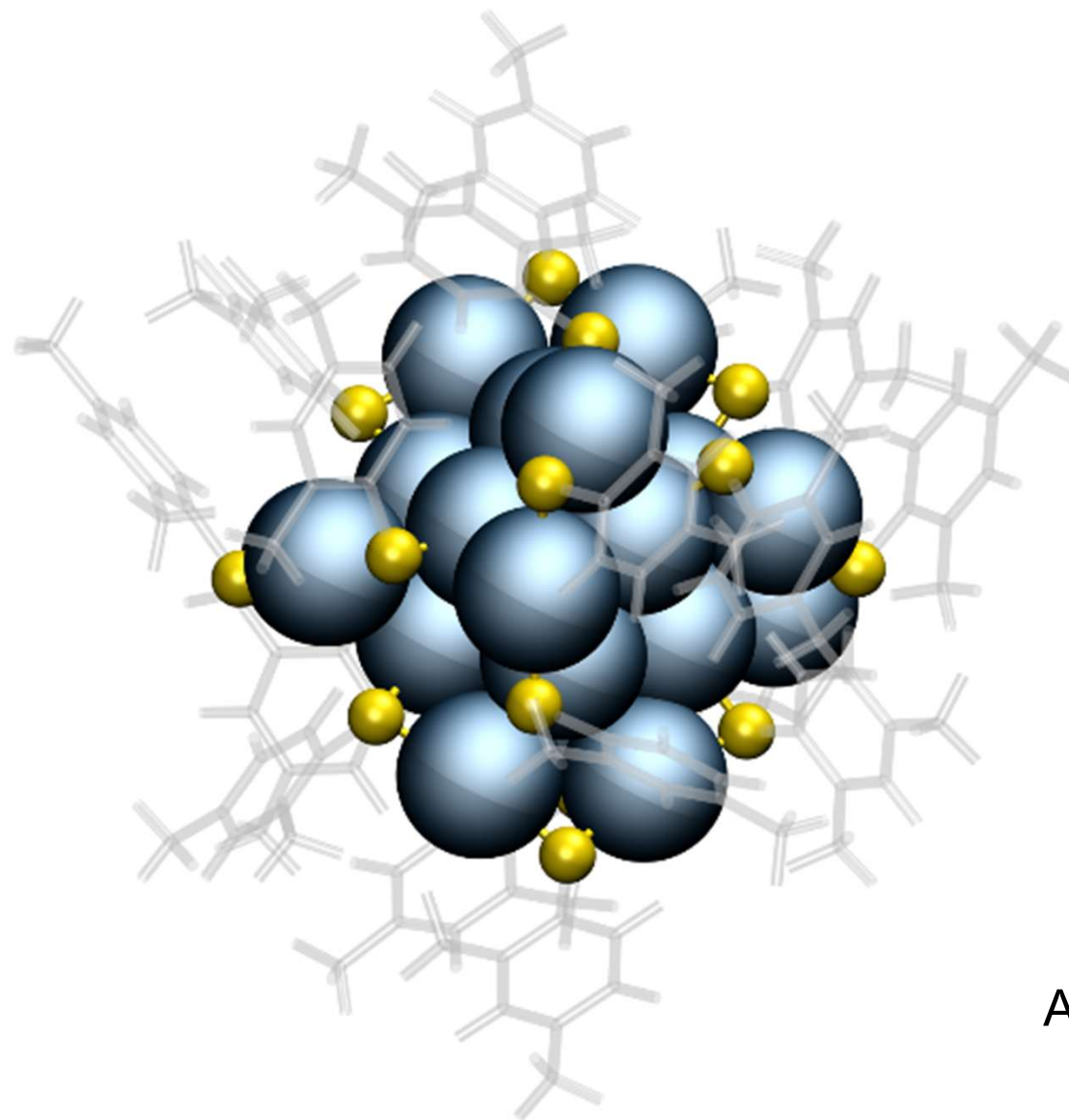


International Centre for Clean Water

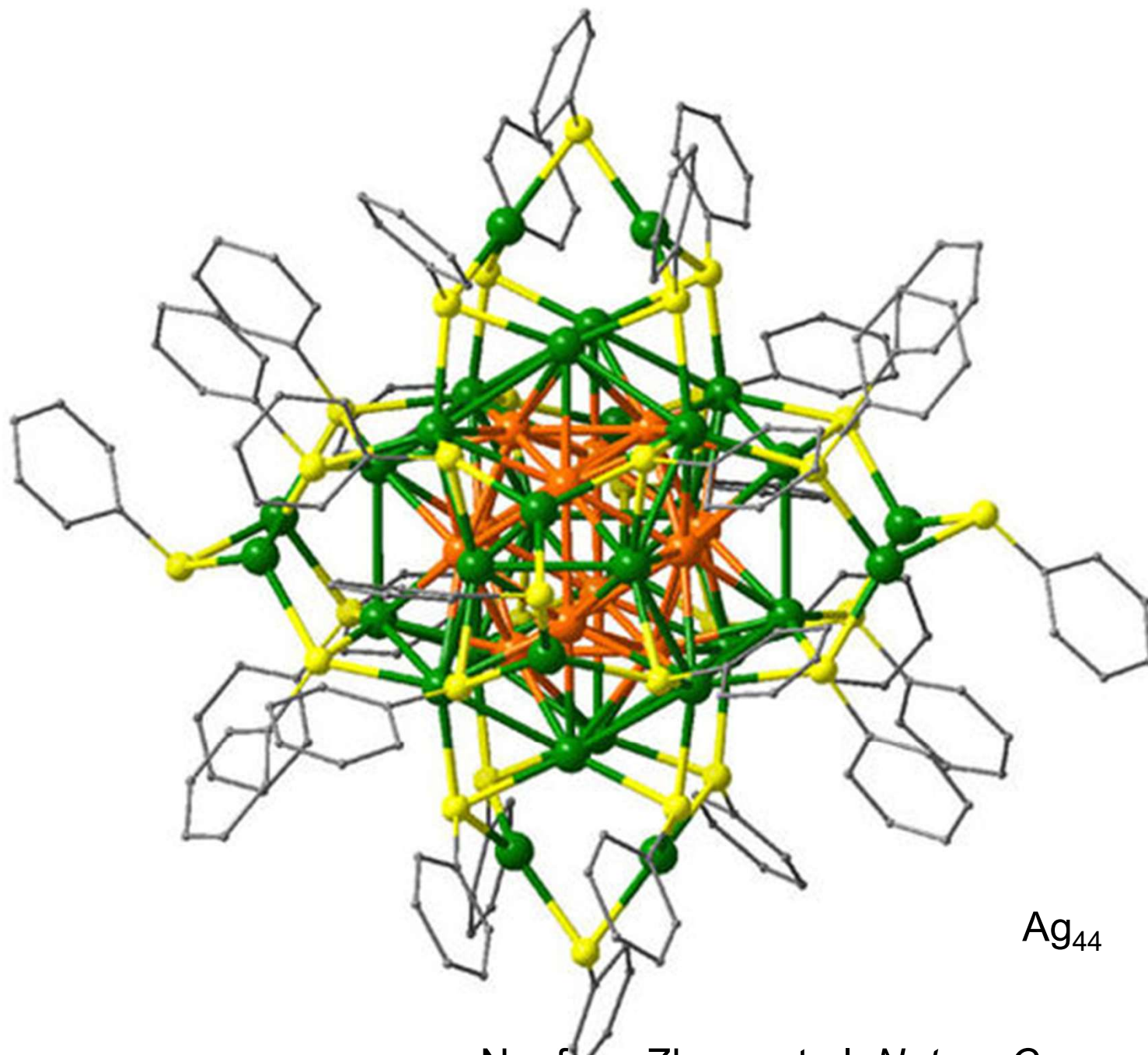


Molecular Materials and Functions - 2022, December 5-7, 2022

New molecules



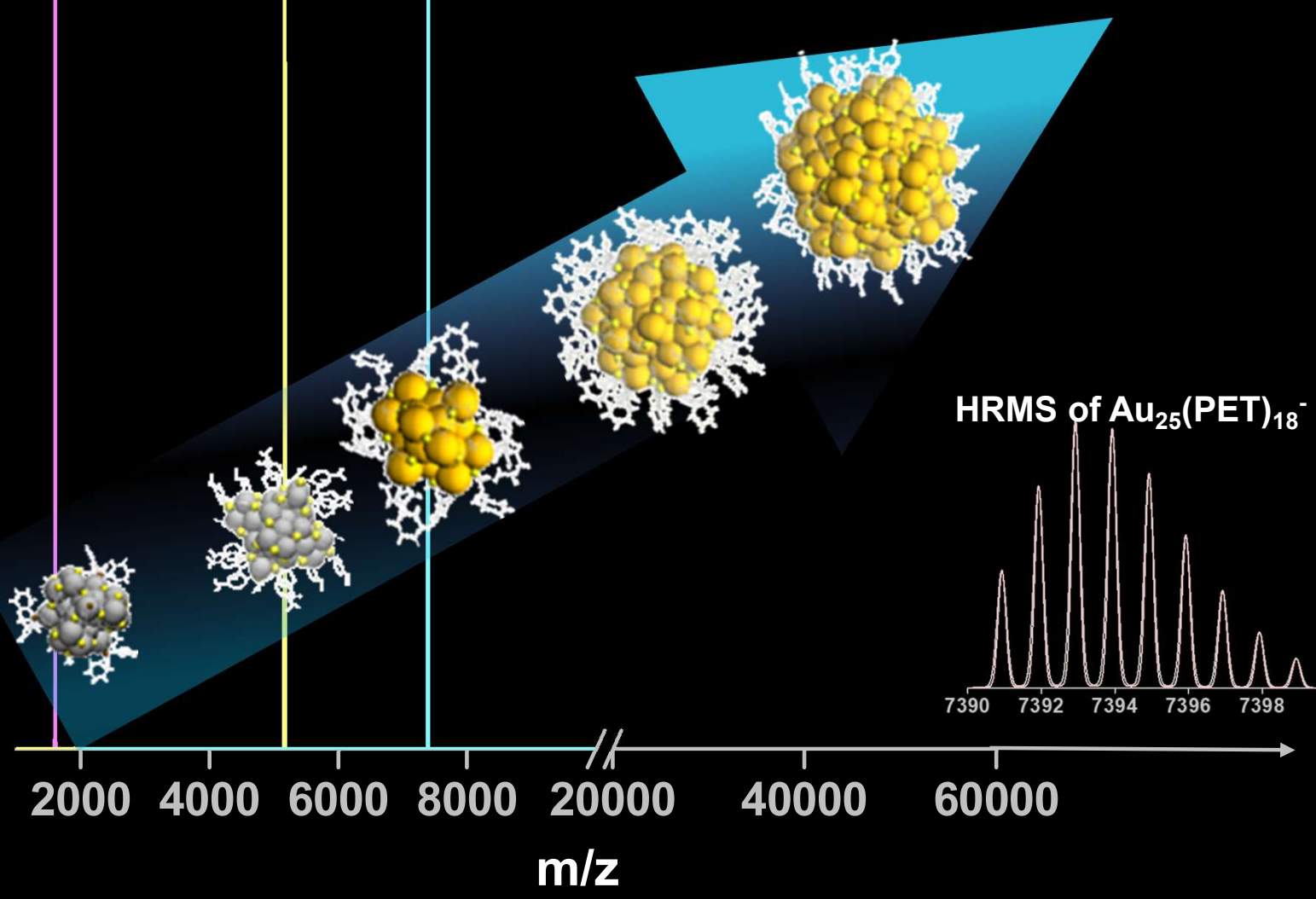
$\text{Au}_{25}, \text{Ag}_{25}, \text{Ag}_{29}$



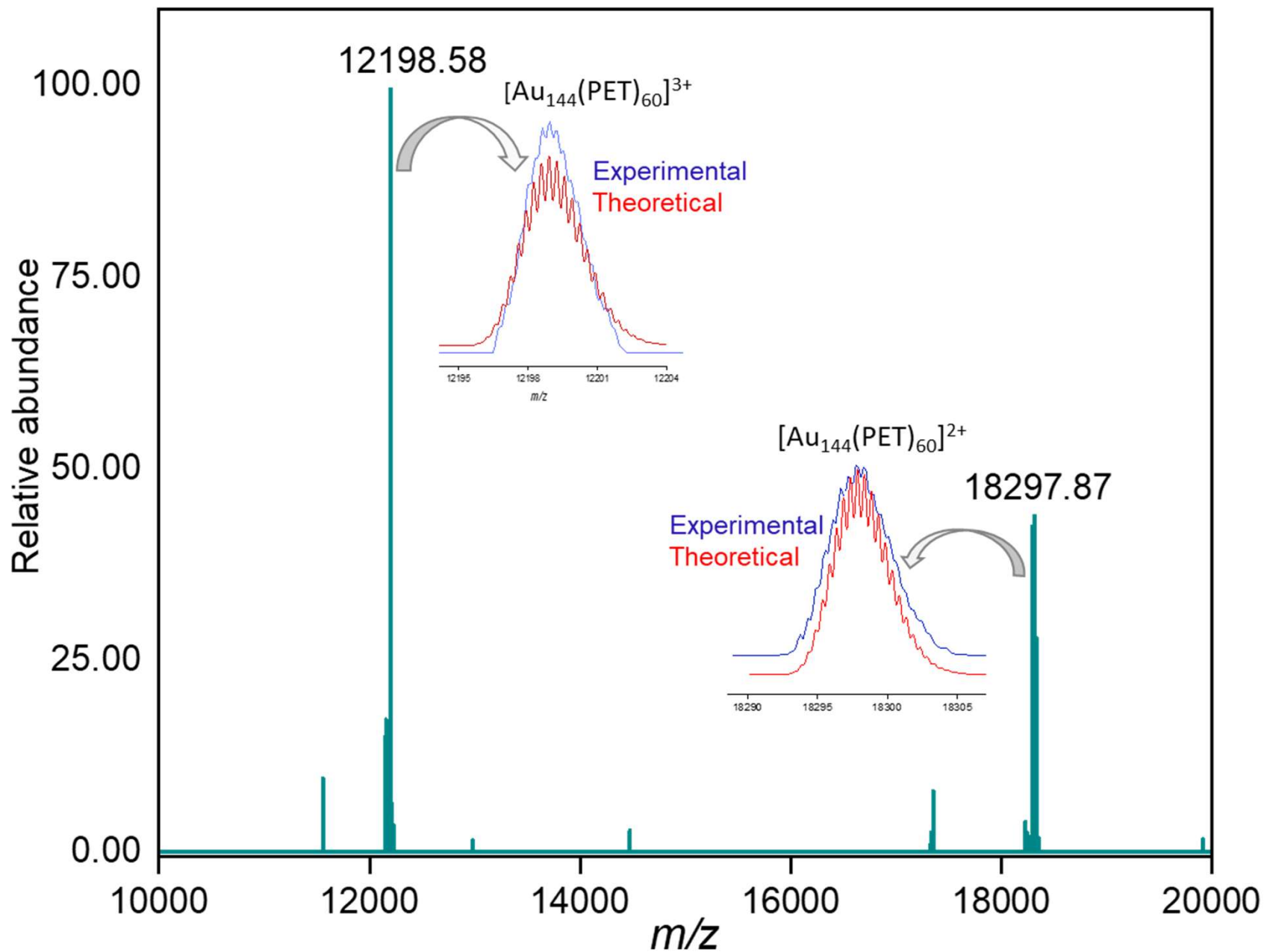
Ag_{44}

Nanfeng Zheng et al. *Nature Communications*, 2013
Terry Bigioni et al. *Nature* 2013

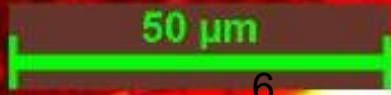
$\text{Ag}_{29}(\text{BDT})_{12}^{3-}$ $\text{Ag}_{25}(\text{DMBT})_{18}^{-}$ $\text{Au}_{25}(\text{PET})_{18}^{-}$



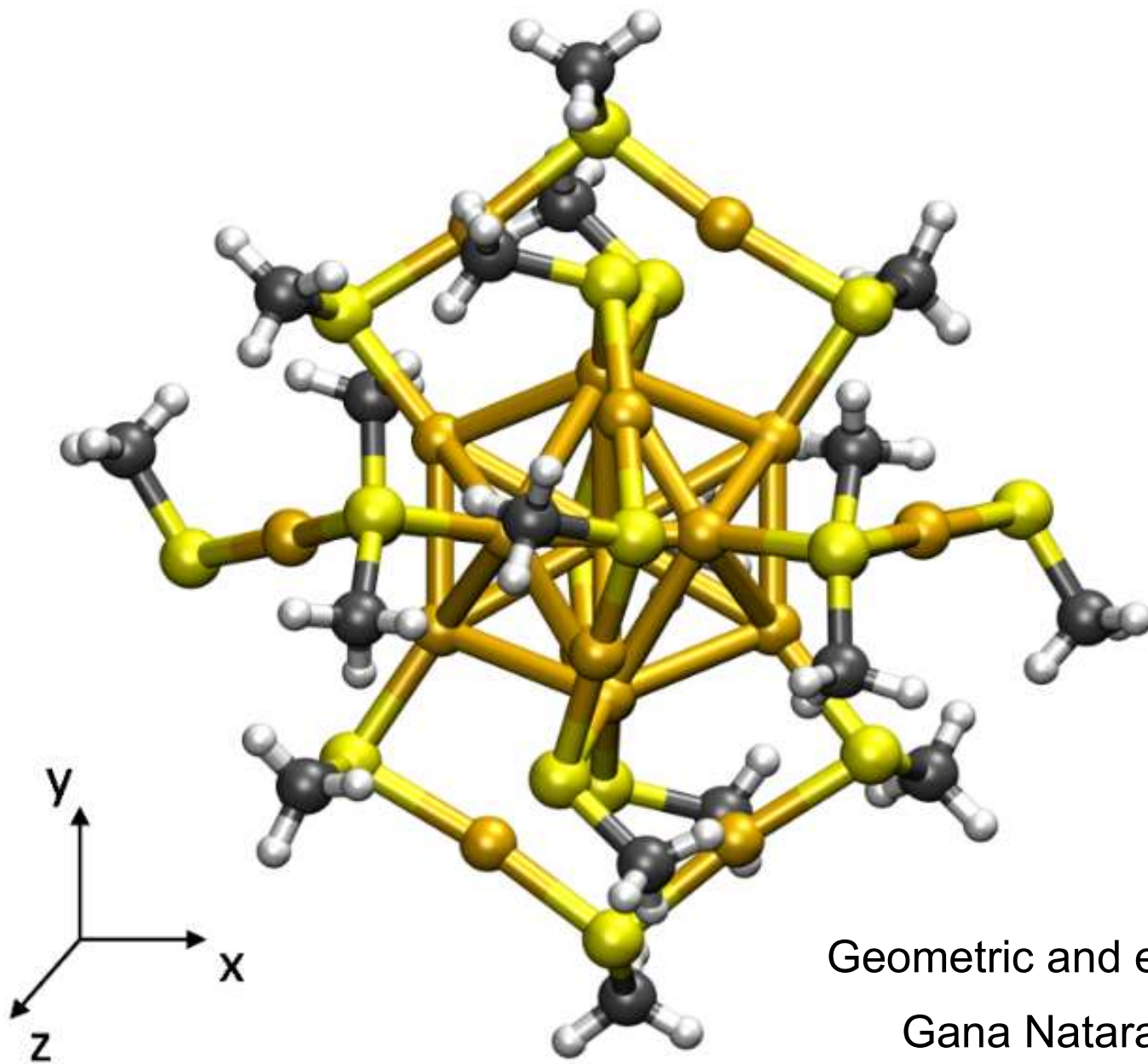
$\text{Au}_{144}(\text{PET})_{60}$



They make high quality crystals



Molecular structure



Geometric and electronic shells

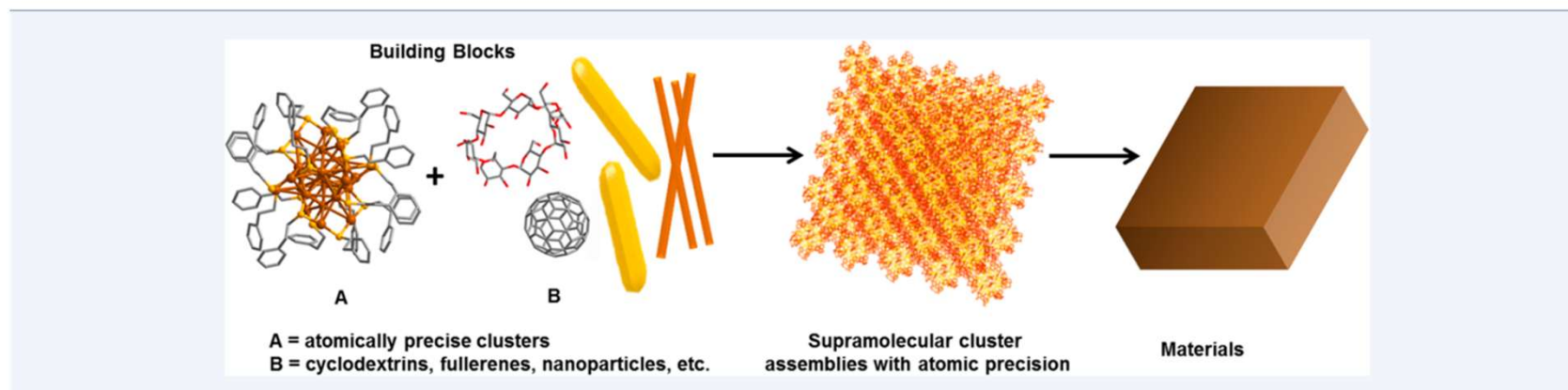
Gana Natarajan

Molecular materials

1 Approaching Materials with Atomic Precision Using Supramolecular 2 Cluster Assemblies 3

4 Papri Chakraborty, Abhijit Nag, Amrita Chakraborty, and Thalappil Pradeep*^{ID}

5 DST Unit of Nanoscience (DST UNS) and Thematic Unit of Excellence (TUE), Department of Chemistry, Indian Institute of
6 Technology Madras, Chennai 600 036, India



Molecules and their properties

Chemical formula	H ₂ O
Molecular weight	18.0148
Critical temperature	373.91°C
Critical pressure	22.05 MPa
Critical density	315.0 kg/m ³
Triple point temperature	0.01°C
Triple point pressure	615.066 Pa
Normal boiling point	100.0°C
Normal freezing point	0.0°C
Density of ice at normal melting point	918.0 kg/m ³
Maximum density, 3.98°C	999.973 kg/m ³
Viscosity, 25°C	0.889 mN s/m ²
Surface tension, 25°C	72 mN/m
Heat Capacity, 25°C	4.1796 kJ/kg.K
Enthalpy of vaporisation, 100°C	2,257.7 kJ/kg
Enthalpy of fusion, 0°C	333.8 kJ/kg
Velocity of sound, 0°C	1.403 km/s
Dielectric constant, 25°C	78.40
Electrical conductivity, 25°C	8 μS/m
Refractive index, 25°C	1.333
Liquid compressibility, 10°C	480. × 10 ⁻¹² m ² /N
Coefficient of thermal expansion, 25°C	256.32 × 10 ⁻⁶ K ⁻¹
Thermal Conductivity, 25°C	0.608 W/m.K

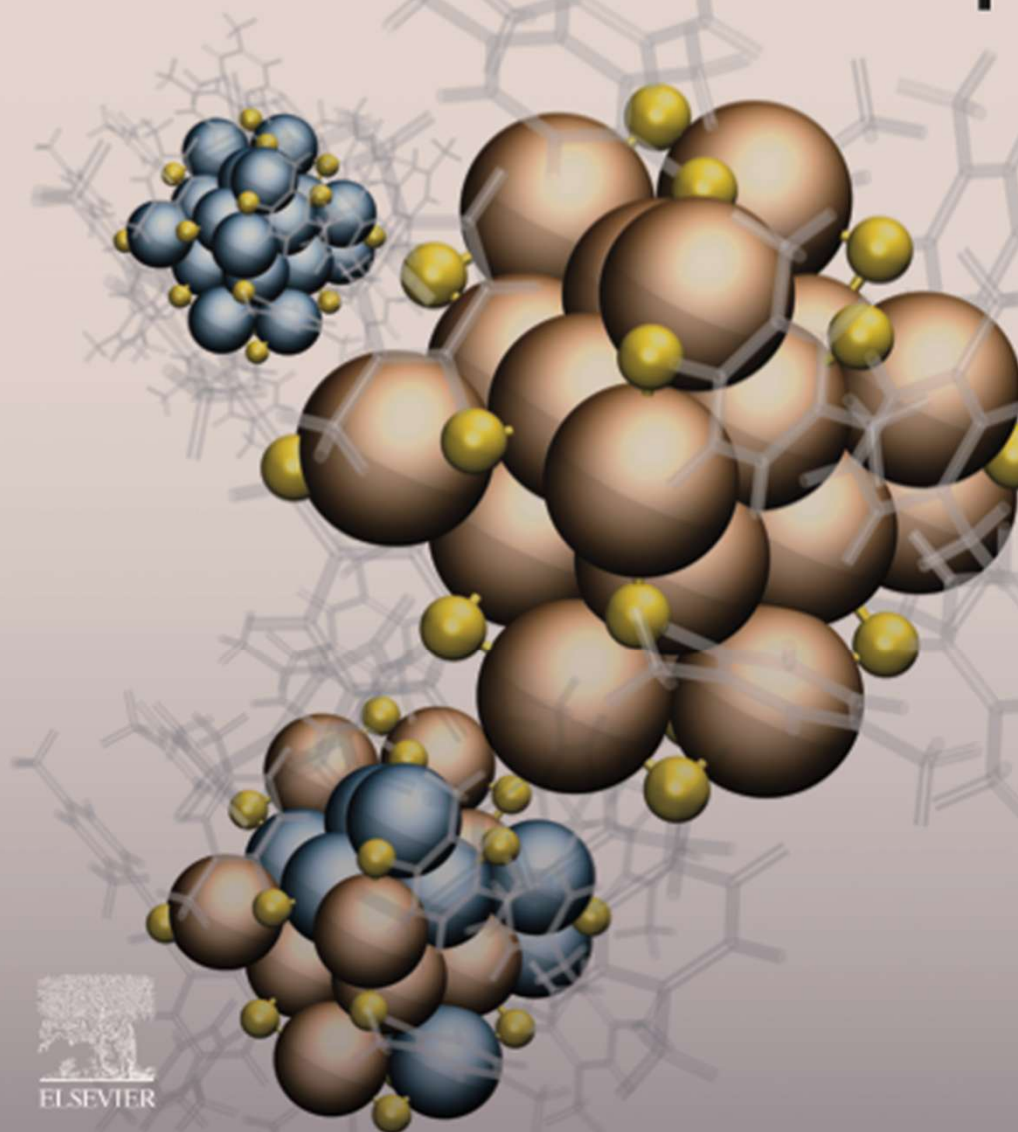
Molecular formula
Molecular weight
Molecular structure
Molecular absorption and emission
Molecular reactions
Molecular assembly
Molecular co-crystals
Ionization potential
Electron affinity

Phases - phase transitions
Physical properties
Electrical, magnetic
Mechanical properties
Electrochemical properties

Future?

Edited by
Thalappil Pradeep

ATOMICALLY PRECISE METAL NANOCCLUSERS



Molecular reactions



Reactions on clusters
Reactions between clusters

Inter-cluster reactions

J | A | C | S
JOURNAL OF THE AMERICAN CHEMICAL SOCIETY

Article

pubs.acs.org/JACS

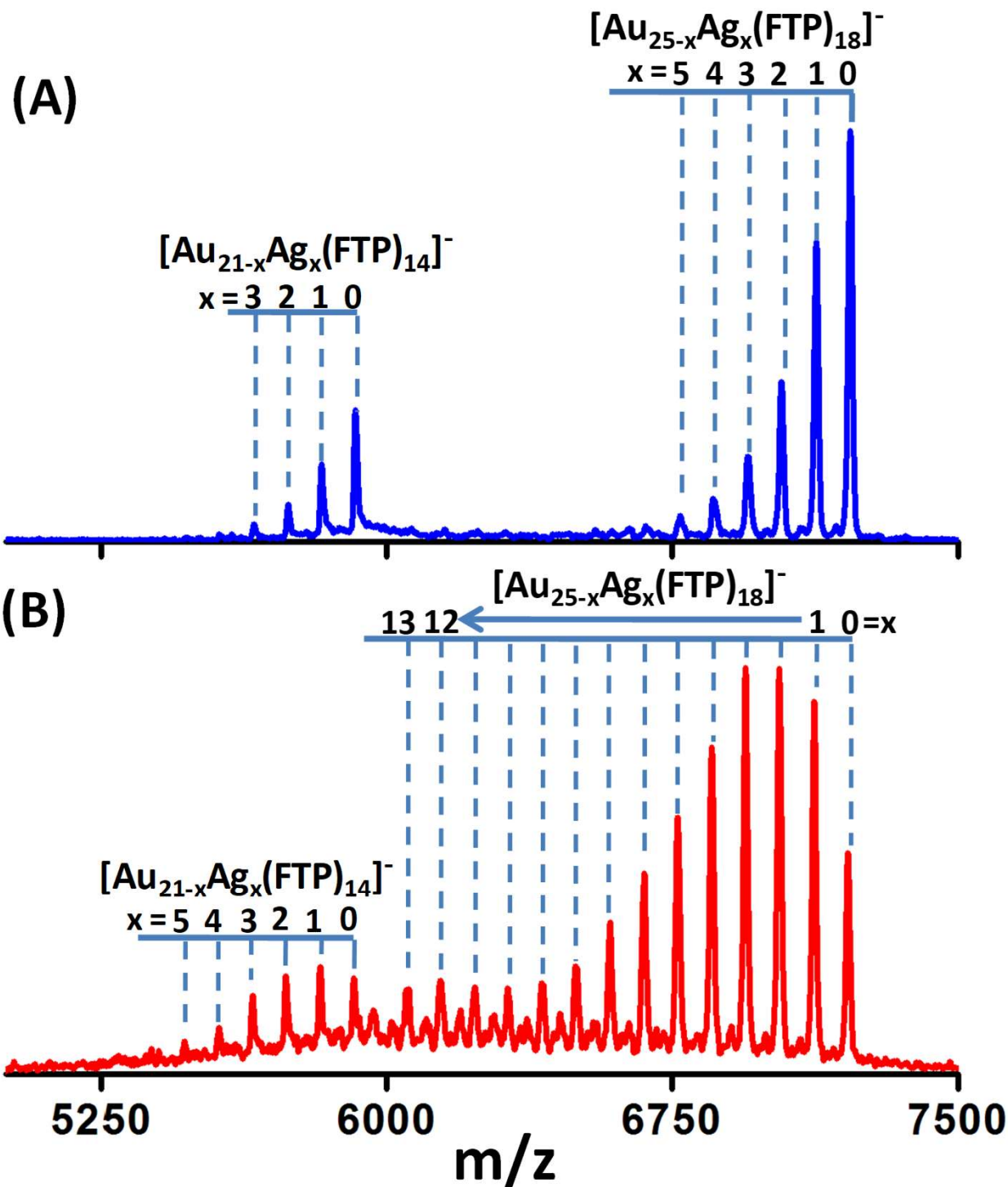
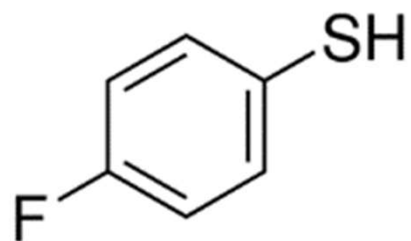
Intercluster Reactions between $\text{Au}_{25}(\text{SR})_{18}$ and $\text{Ag}_{44}(\text{SR})_{30}$

K. R. Krishnadas, Atanu Ghosh, Ananya Baksi, Indranath Chakraborty,[†] Ganapati Natarajan,
and Thalappil Pradeep*

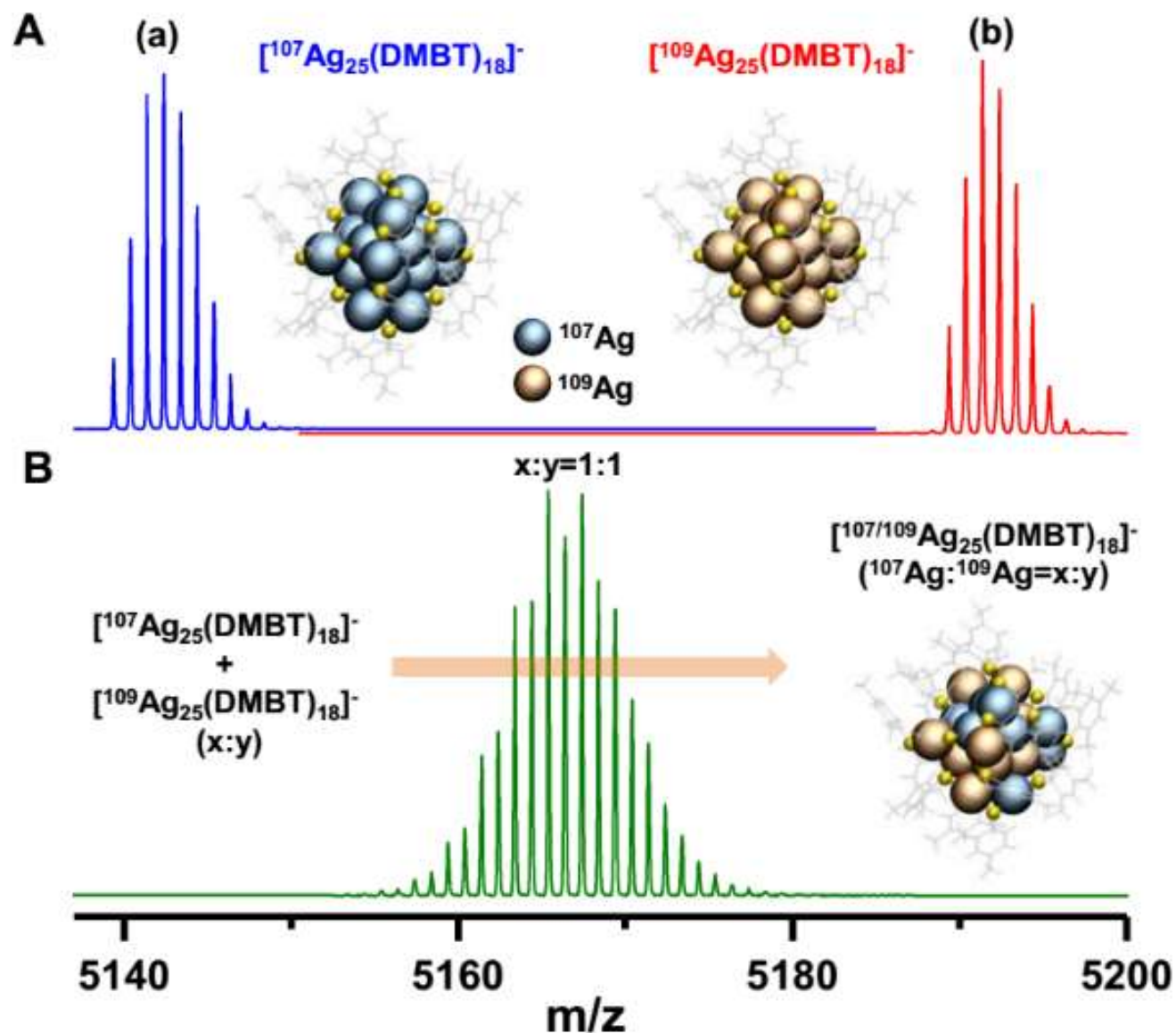
DST Unit of Nanoscience (DST UNS) and Thematic Unit of Excellence, Department of Chemistry, Indian Institute of Technology
Madras, Chennai, 600 036, India

 Supporting Information



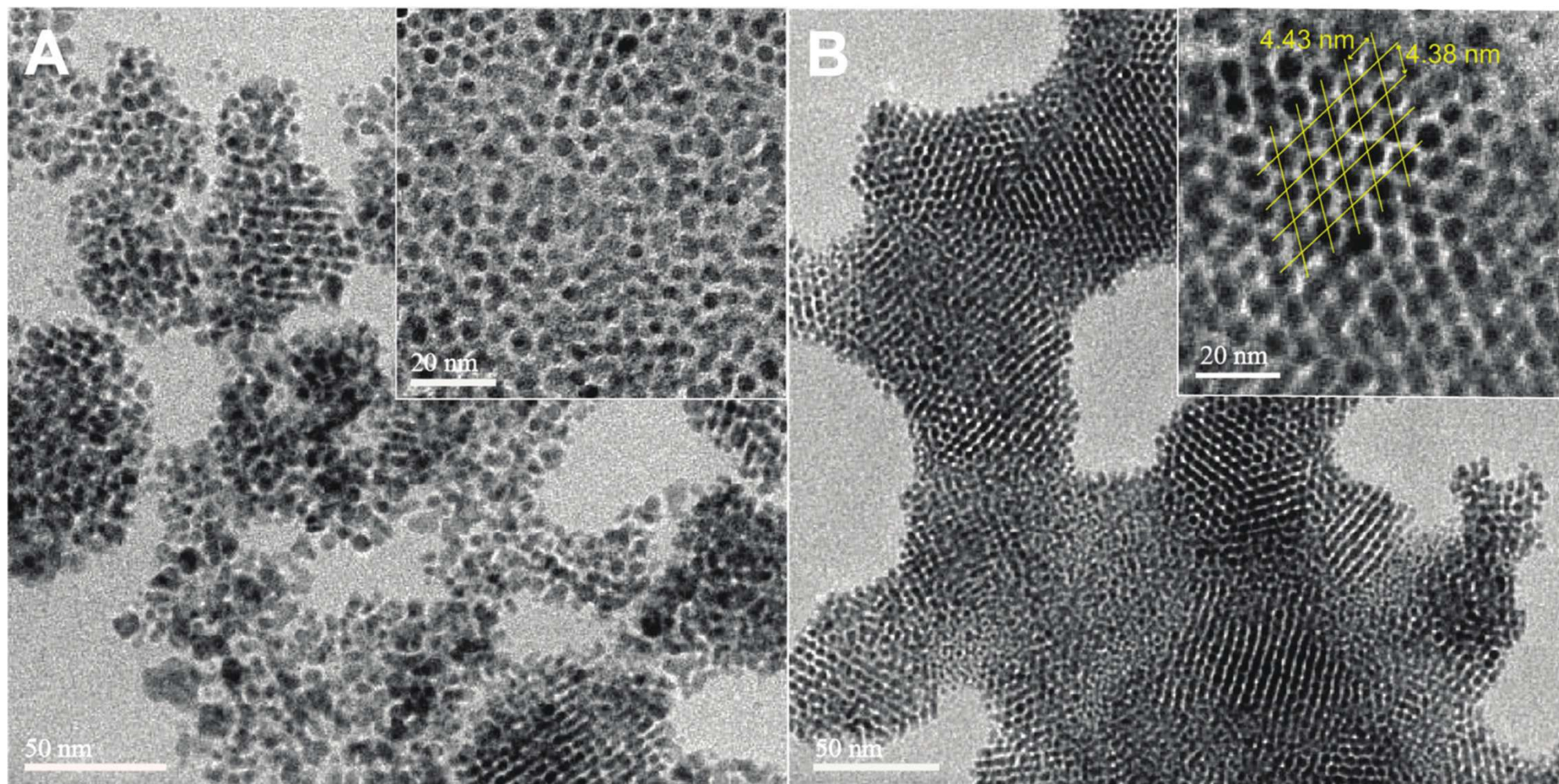


Isotopic exchange



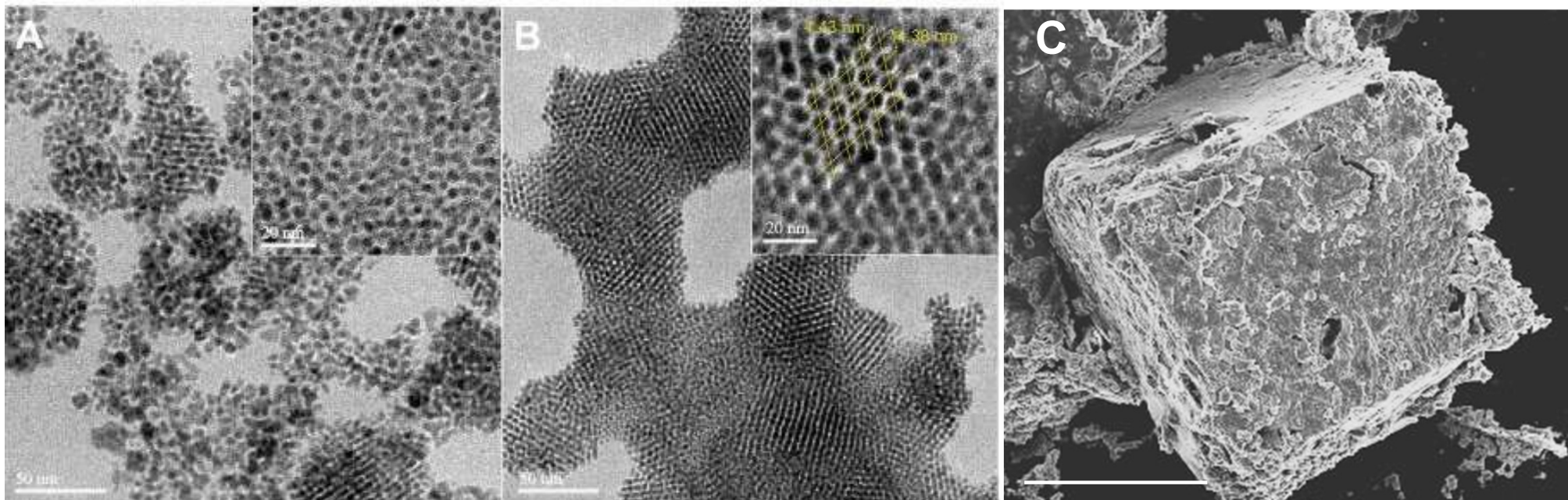
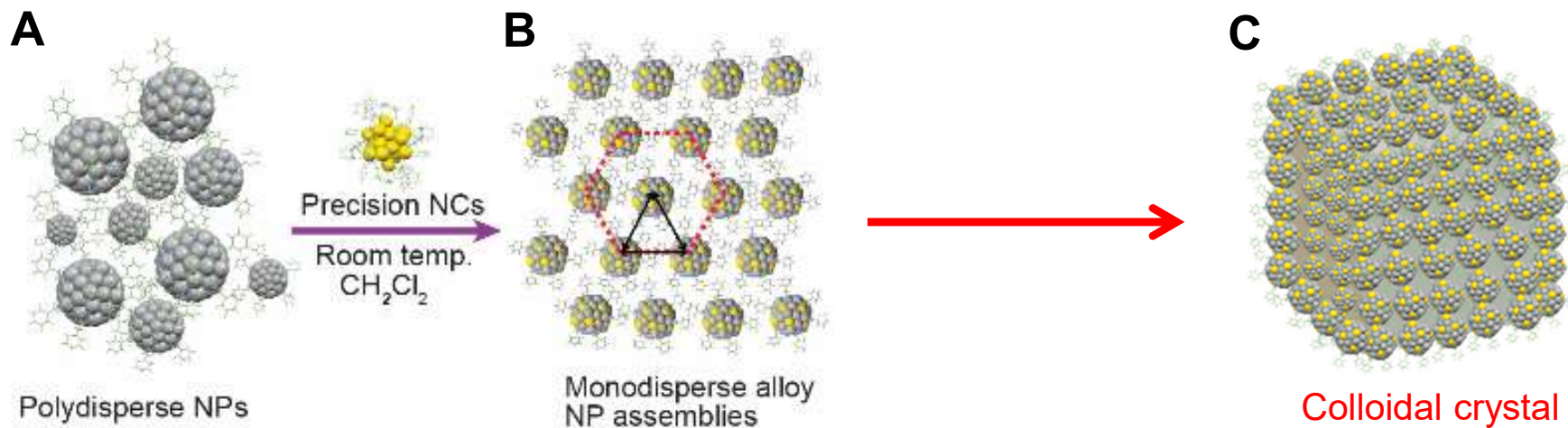
Papri Chakraborti, et. al. Science Advances, 2019.

Chemistry in bulk

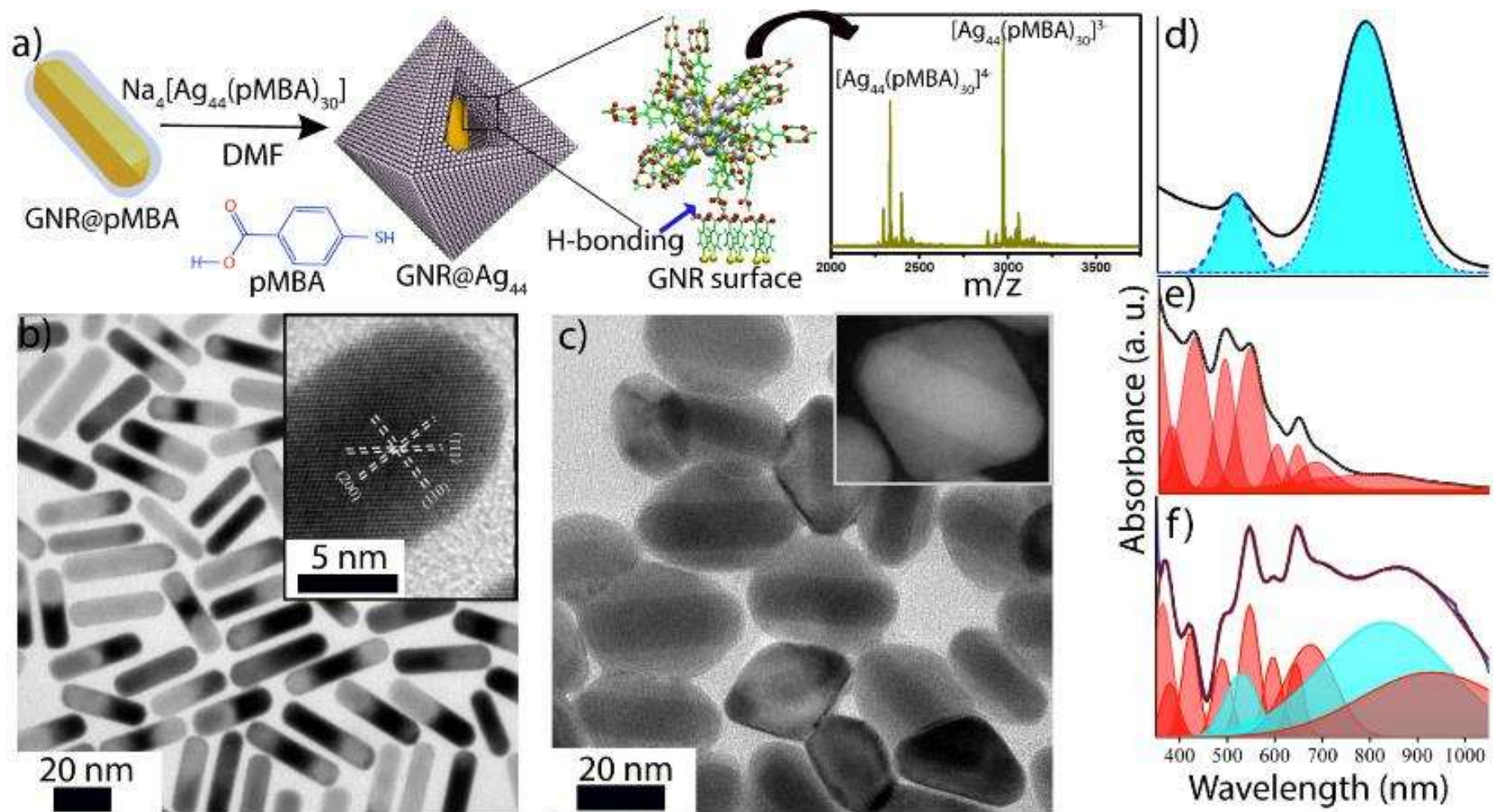


Paulami Bose et al. *Nanoscale* 2020

Crystallization of AgAu NP

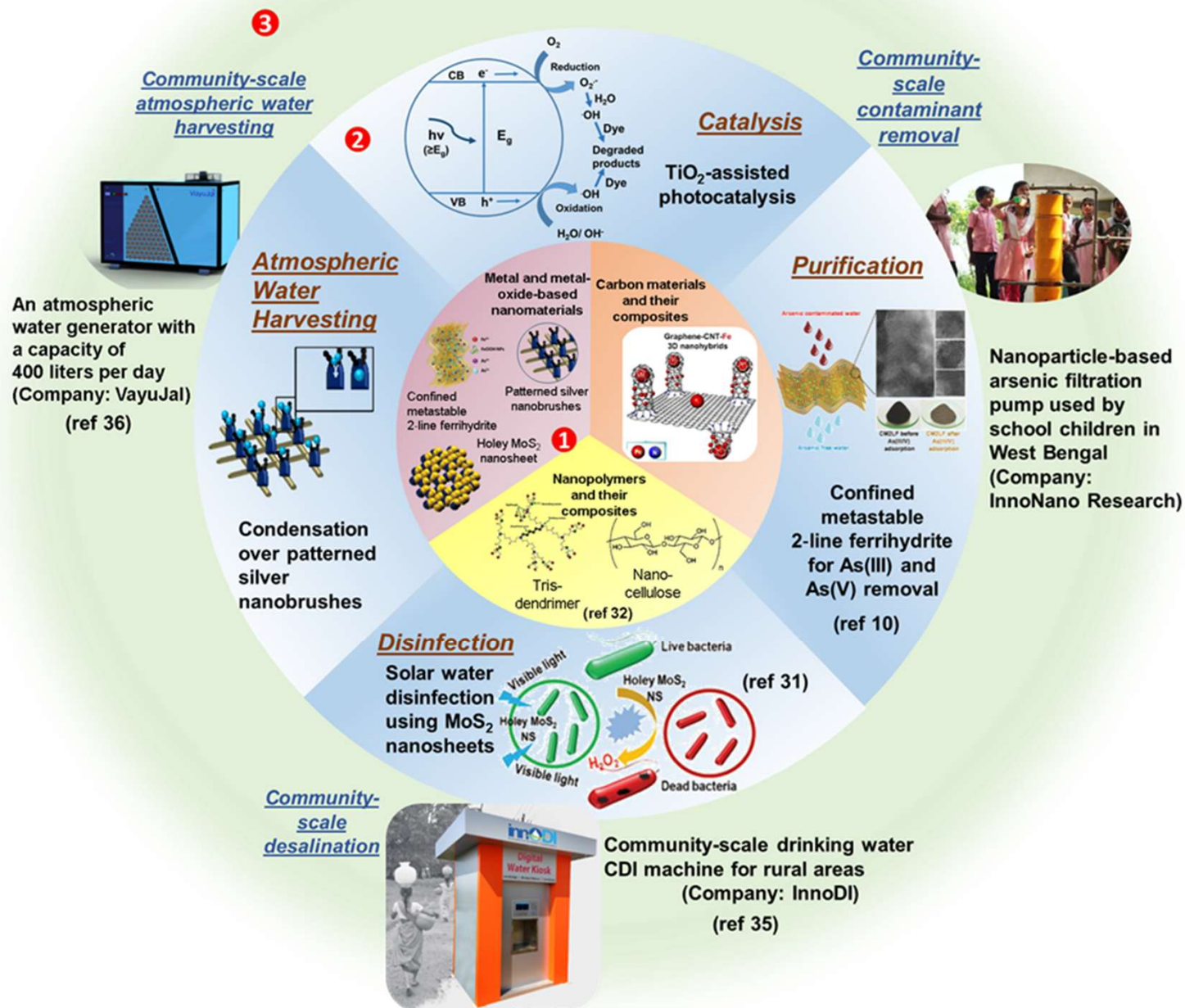


Atomically precise nanocluster assemblies encapsulating plasmonic gold nanorods



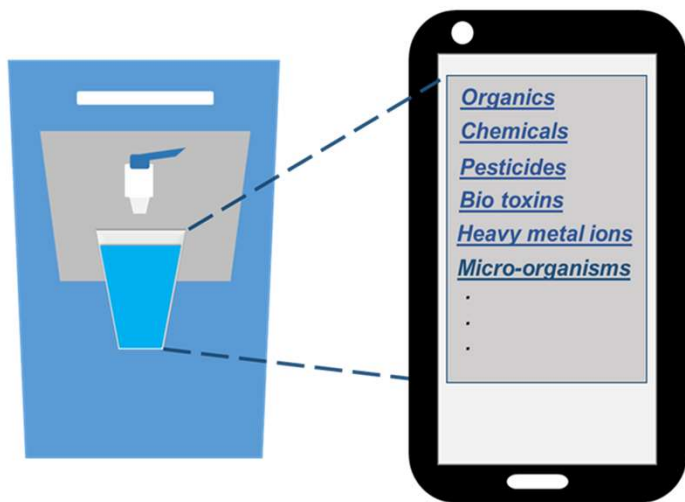
Chakraborty, A. et al., *Angew. Chem. Int. Ed.* 2018, 57, 6522–6526.

Evolution of materials to products

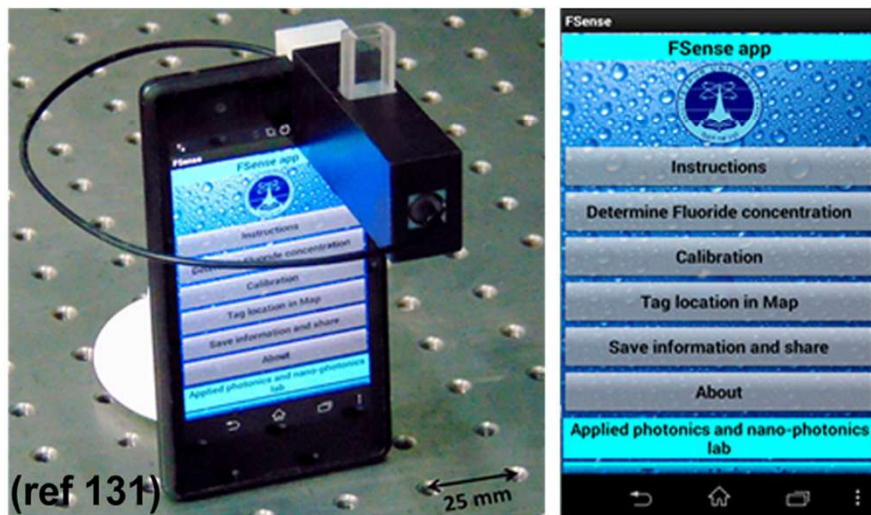


Smart water purifiers and big data

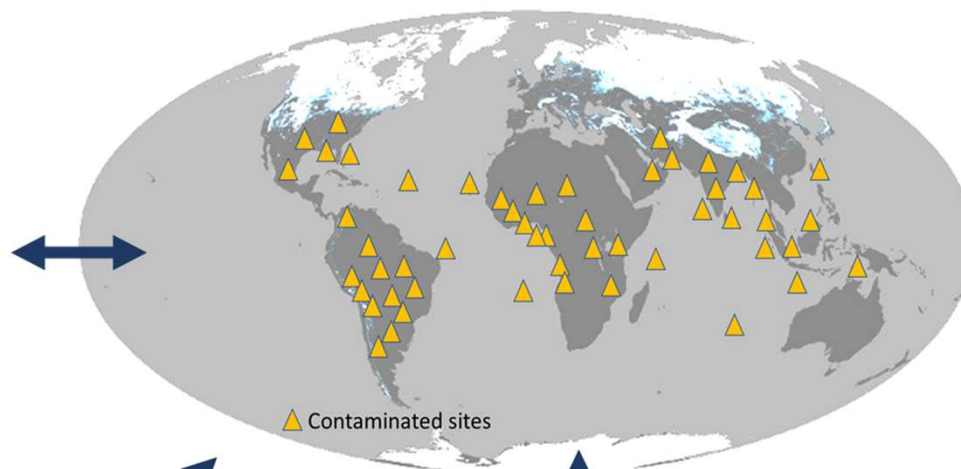
Smart Water Purifiers linked to IoT



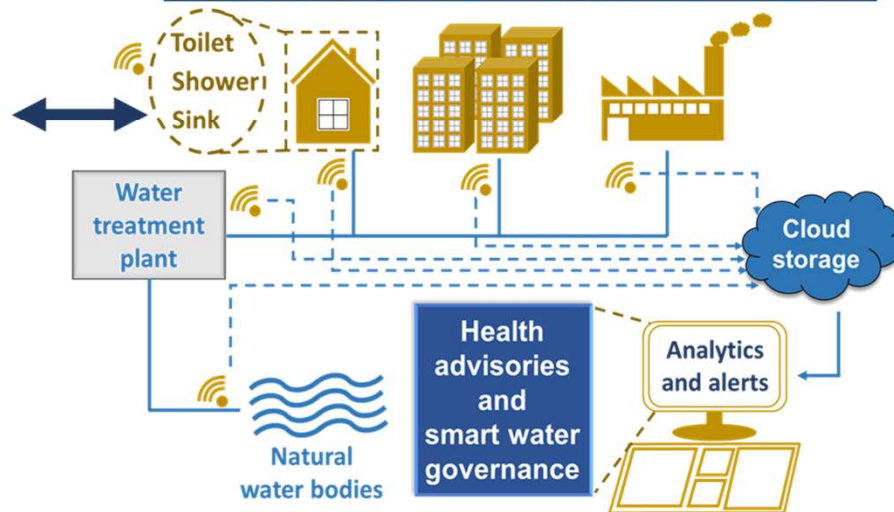
Cost-effective sensor accessory for point-of-use applications



Global Map of Water Health



IoT-enabled sensing for households and distribution networks

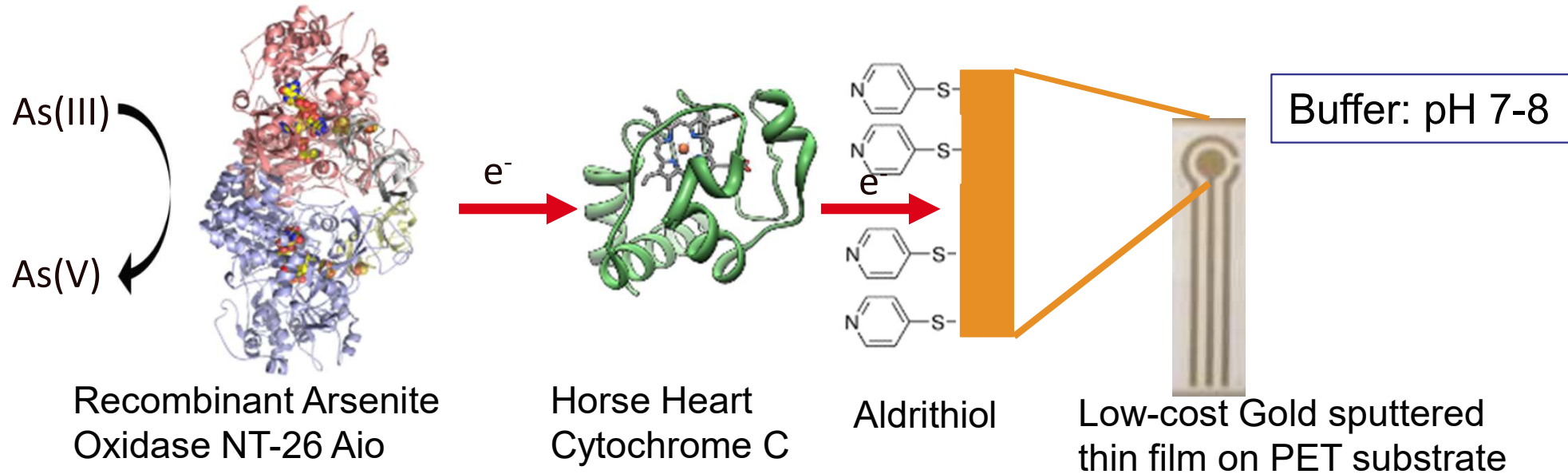


Translation to industry

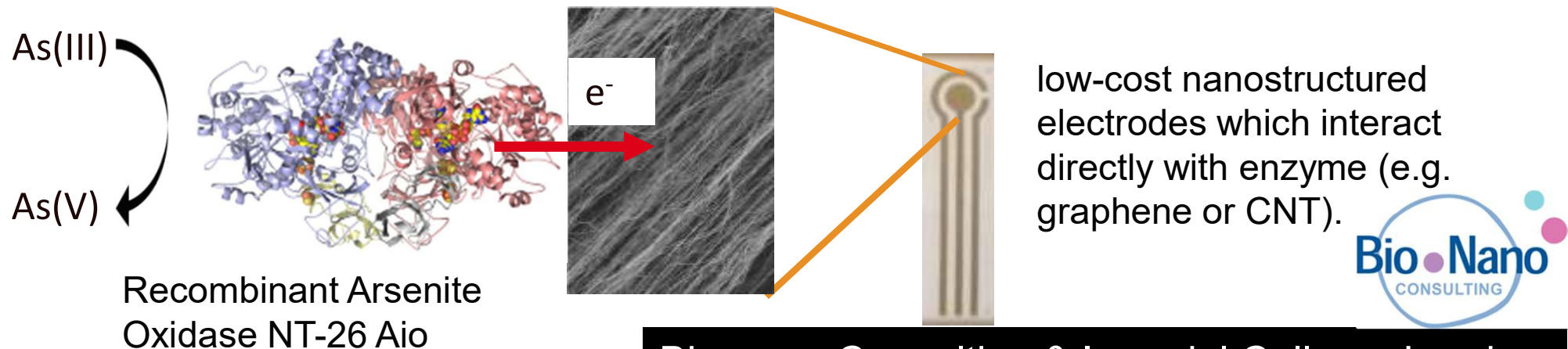


Biosensor Design

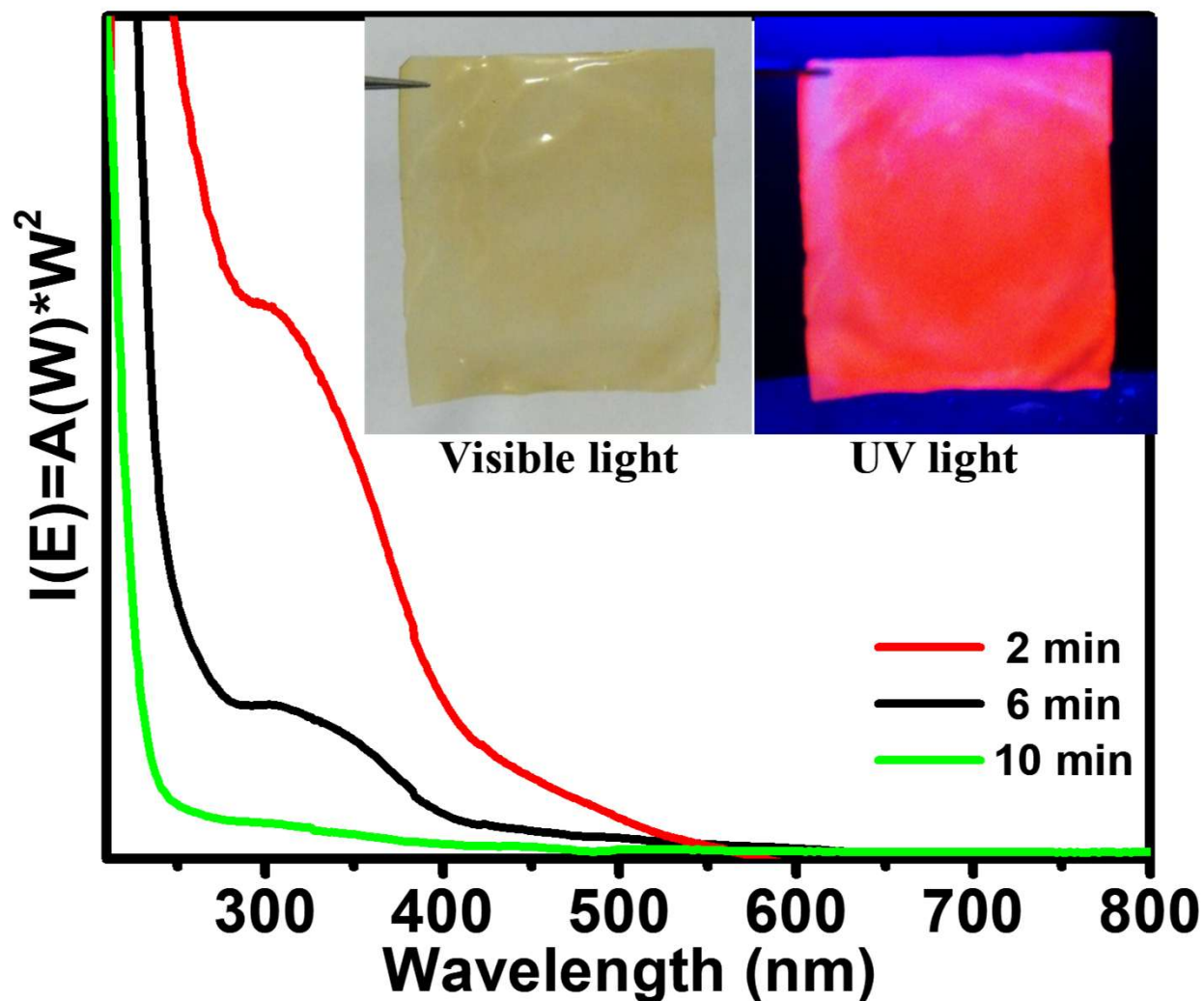
1st Generation Design (Mediated Electrochemistry)



2nd Generation Design (Direct Electron Transfer)

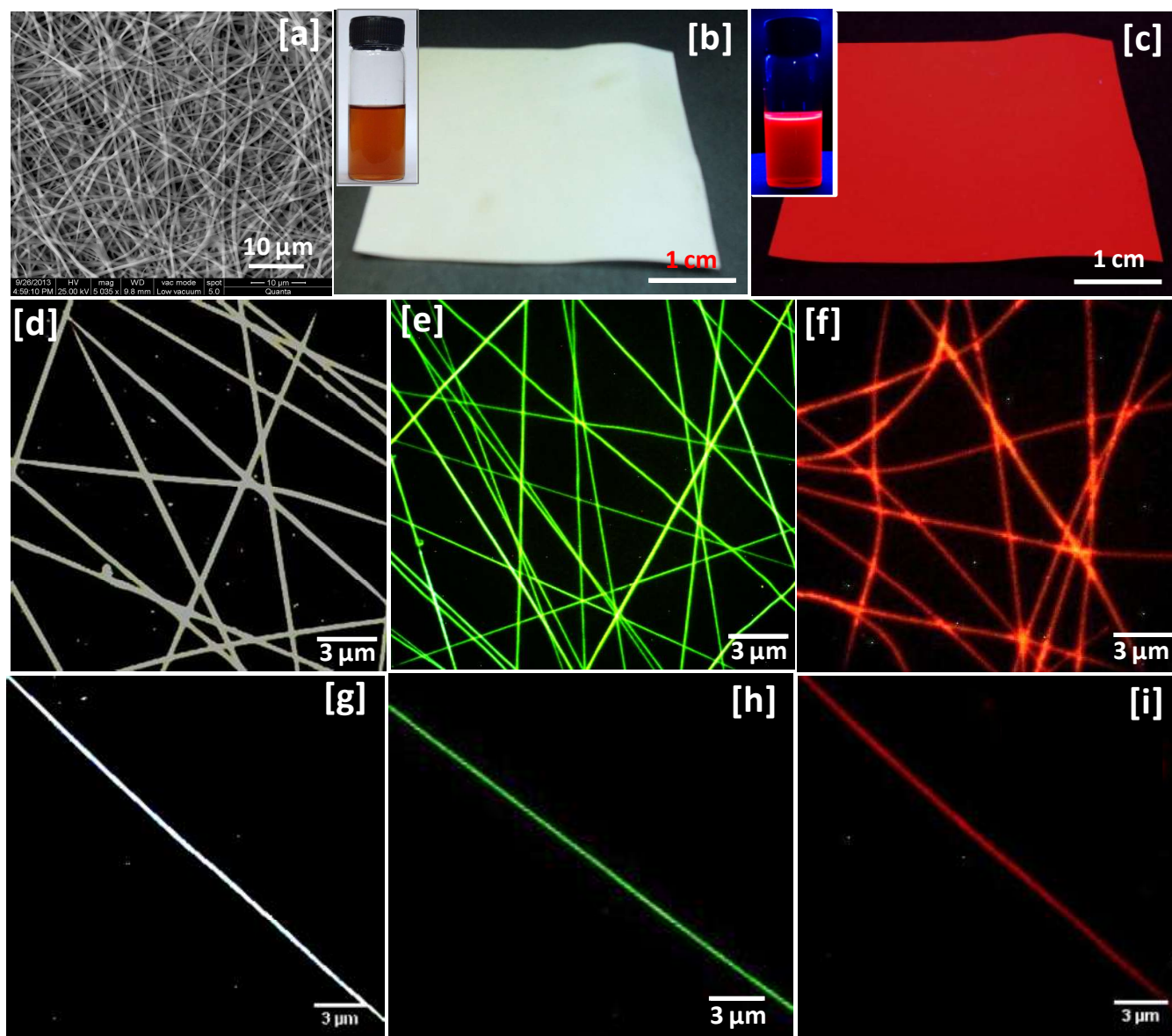


Cluster-based metal ion sensing



Decrease in the absorption of Au_{15} as a biofilm is dipped into the cluster solution. Inset: Free standing quantum cluster loaded film in visible light and UV light.

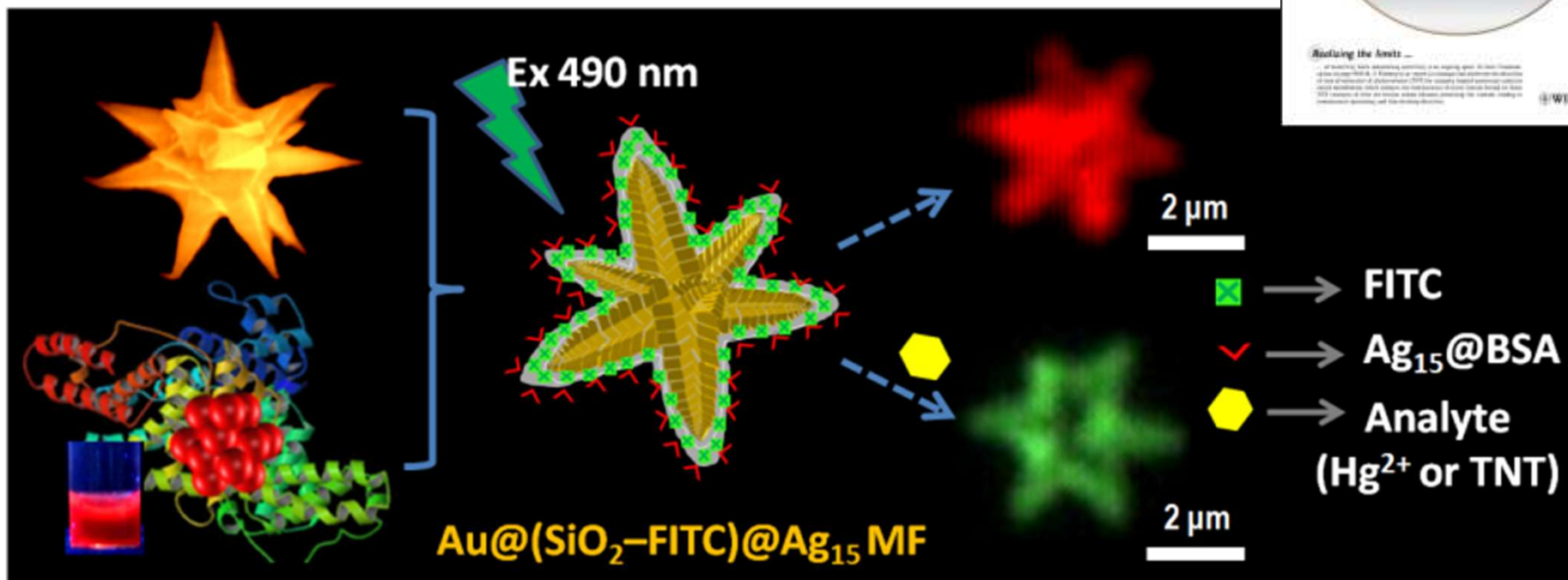
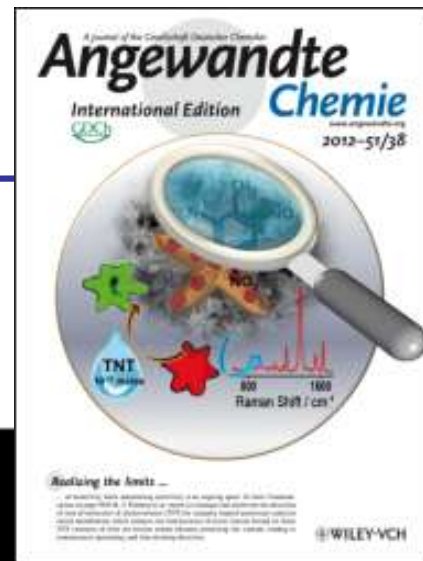
Approaching detection limits of tens of Hg^{2+}



Mercury quenching experiment using nanofiber

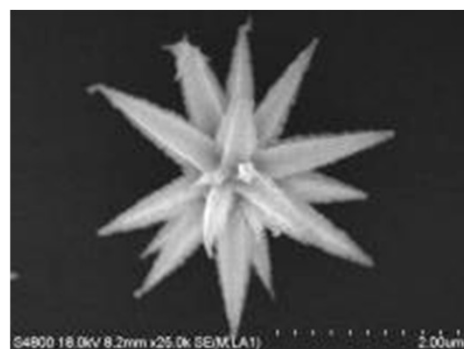


Sub-zeptomolar detection



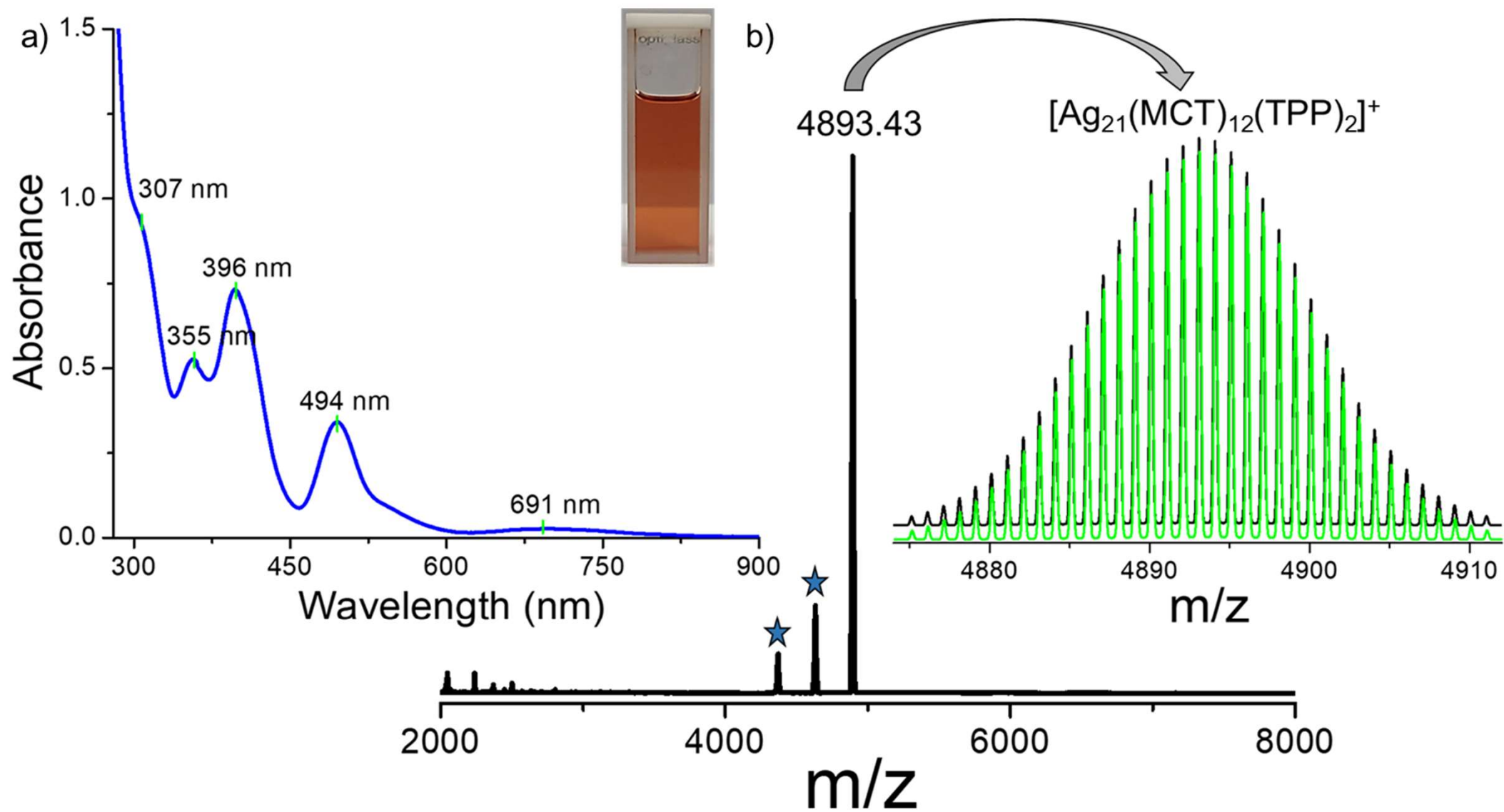
Featured in:

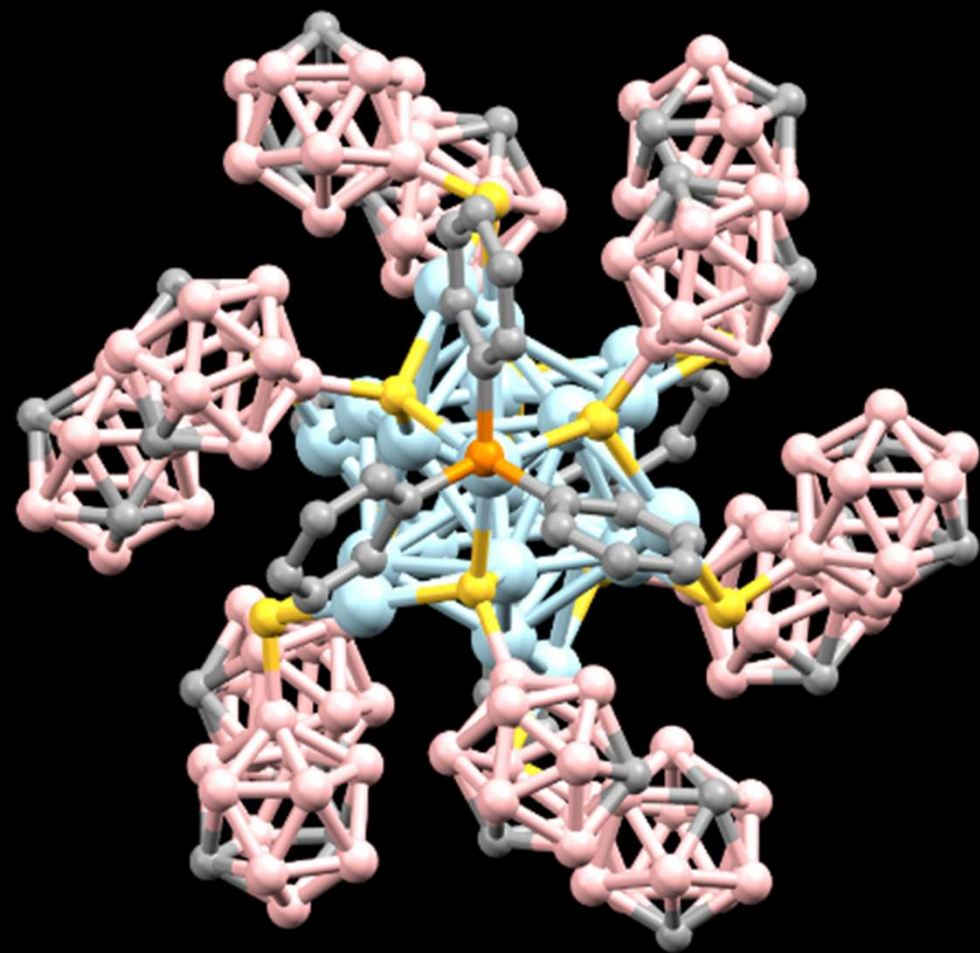
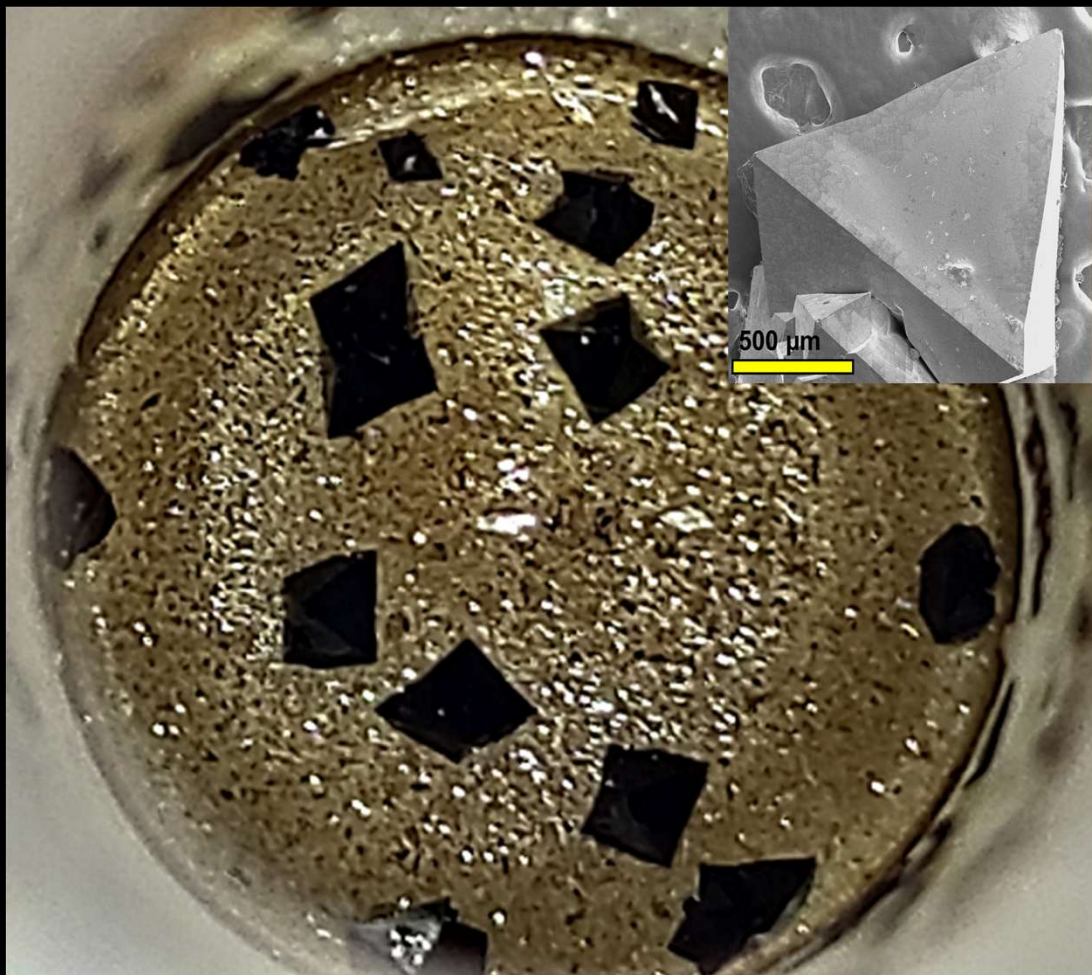
The Hindu, Telegraph, Times of India, etc.
C&E News
and many others



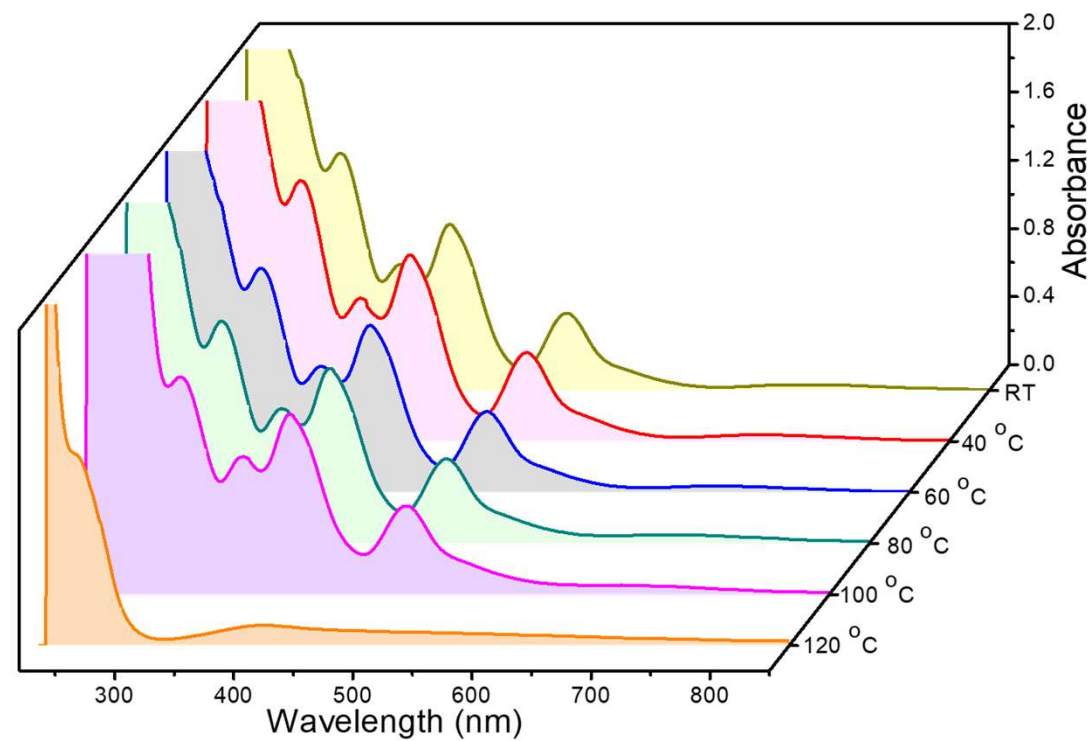
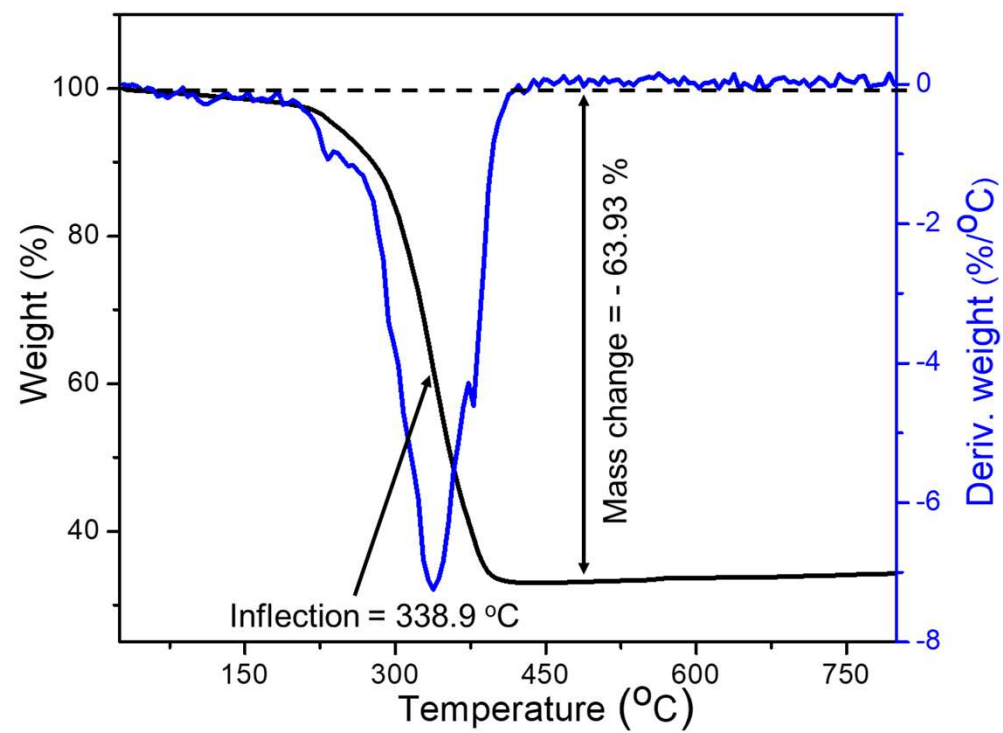
Ammu Mathew, et al. Angew. Chem. Int. Ed. 2012

Characterization of Ag₂₁

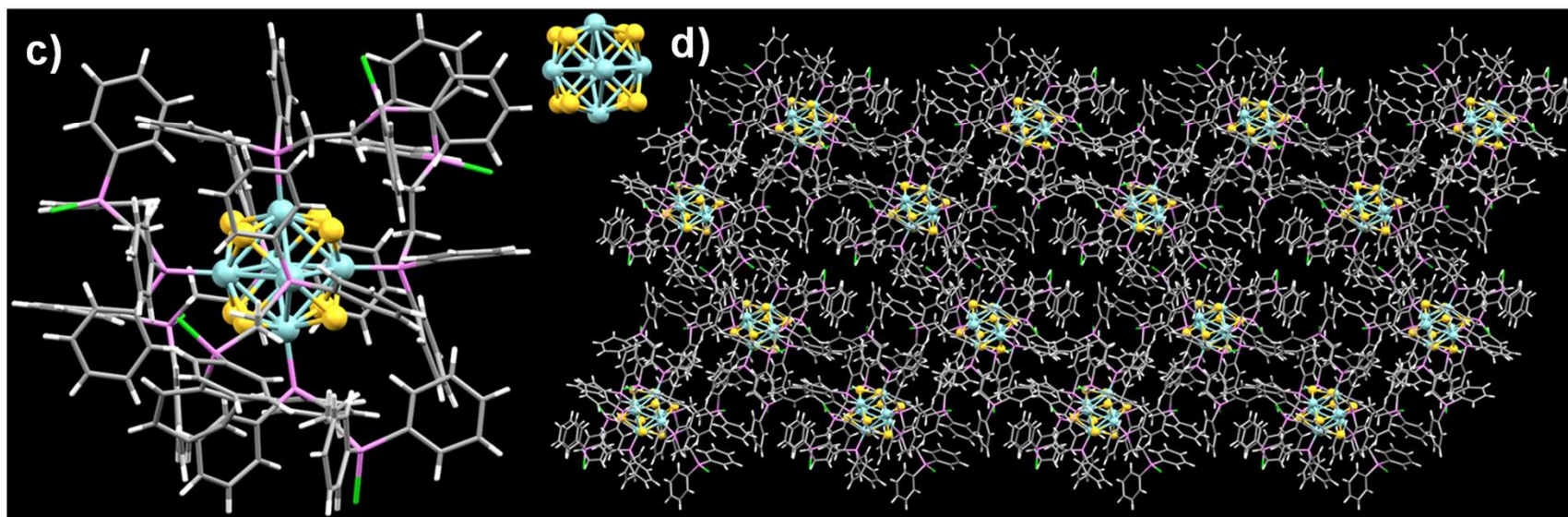
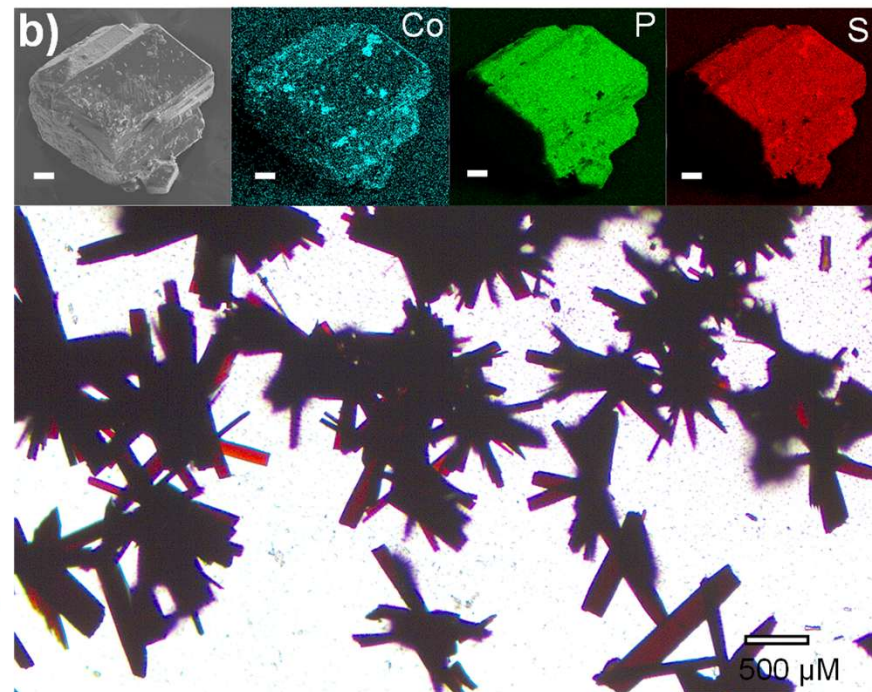
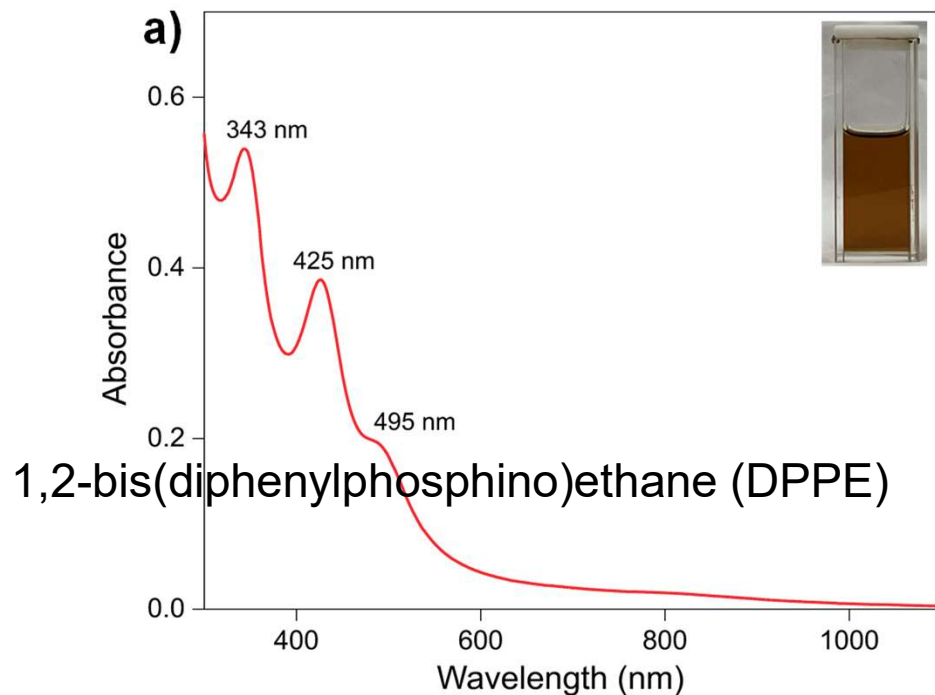




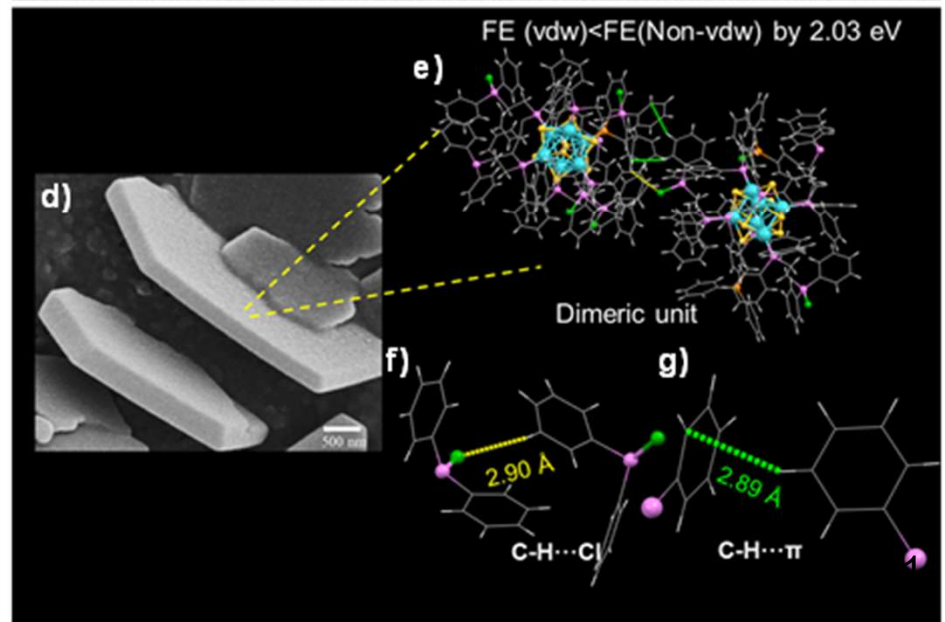
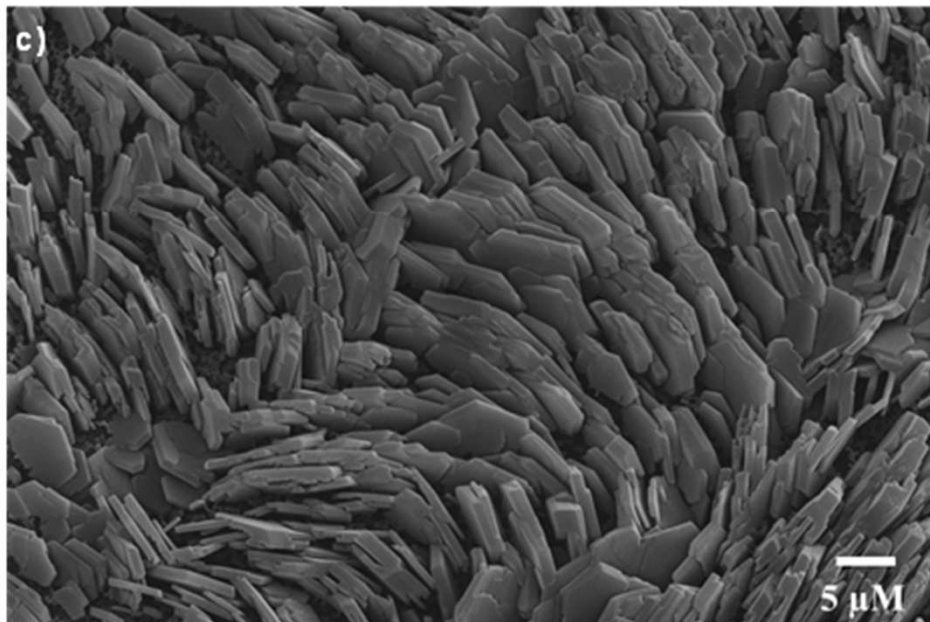
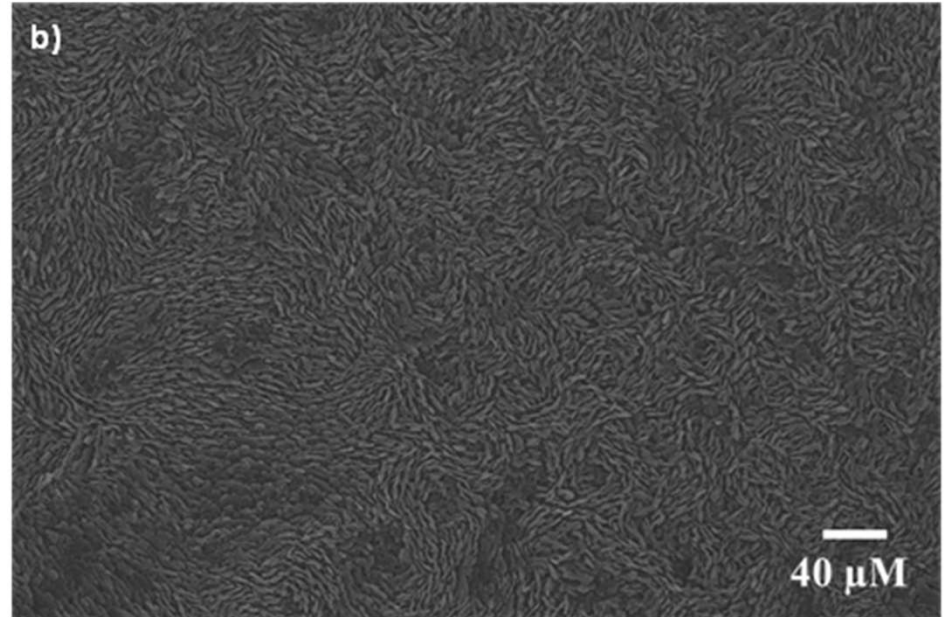
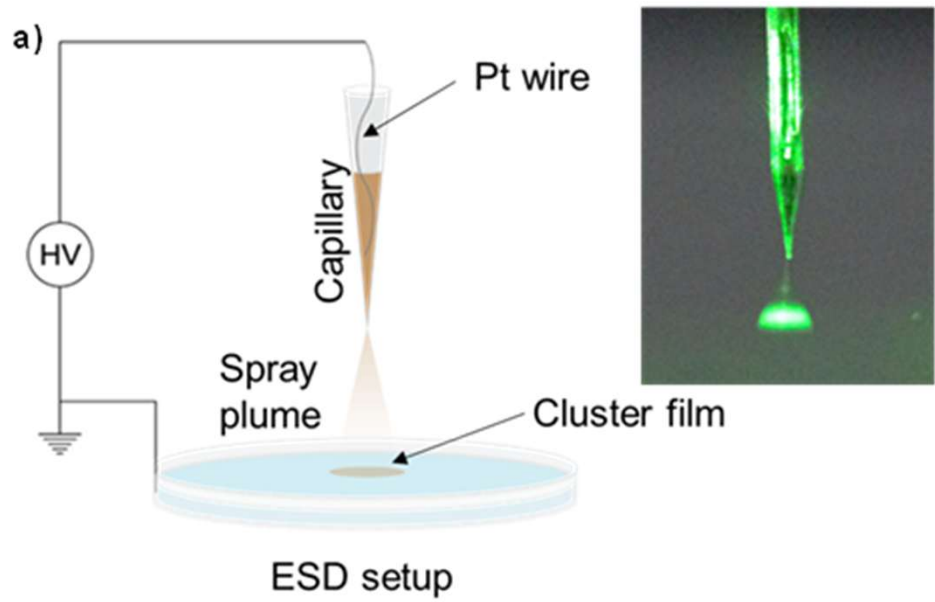
Thermal stability



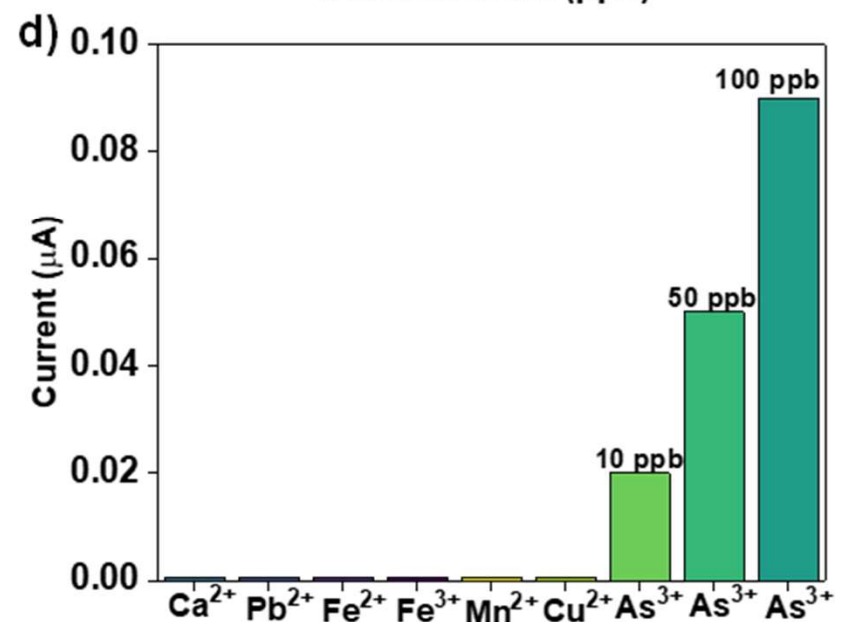
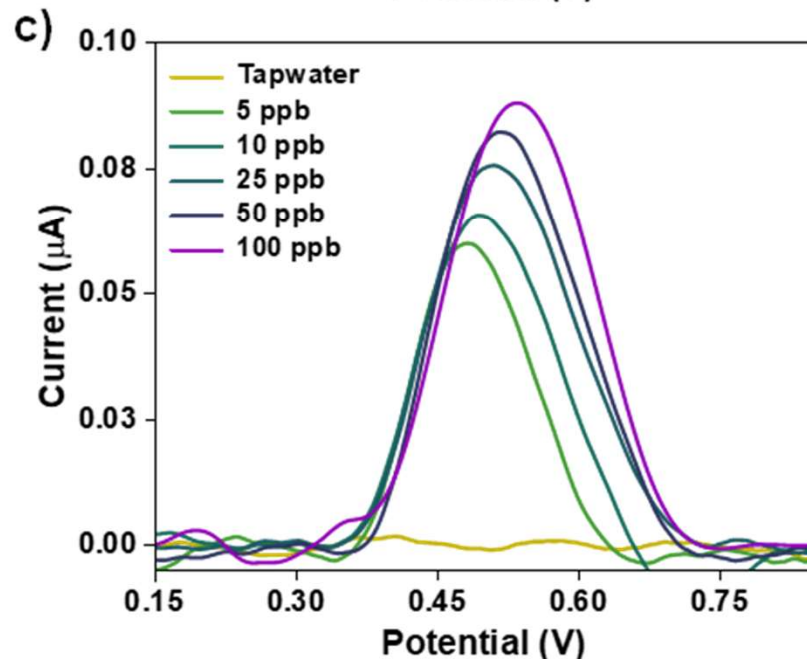
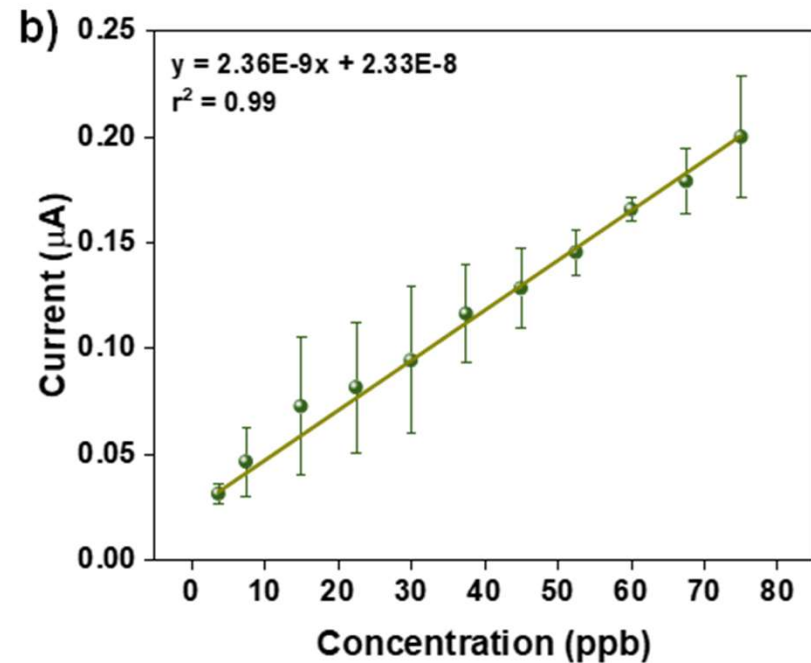
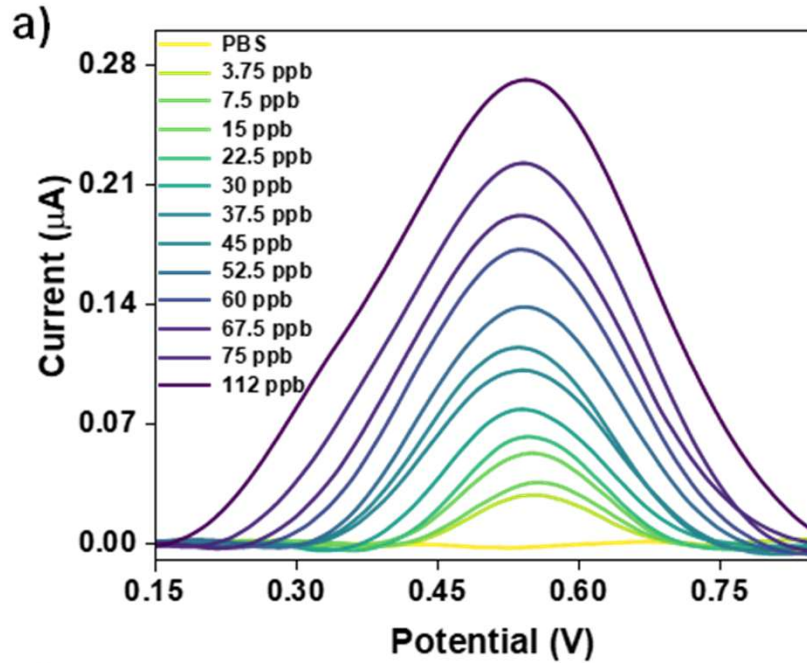
New electrodes - Aligned nanoplates of Co_6S_8



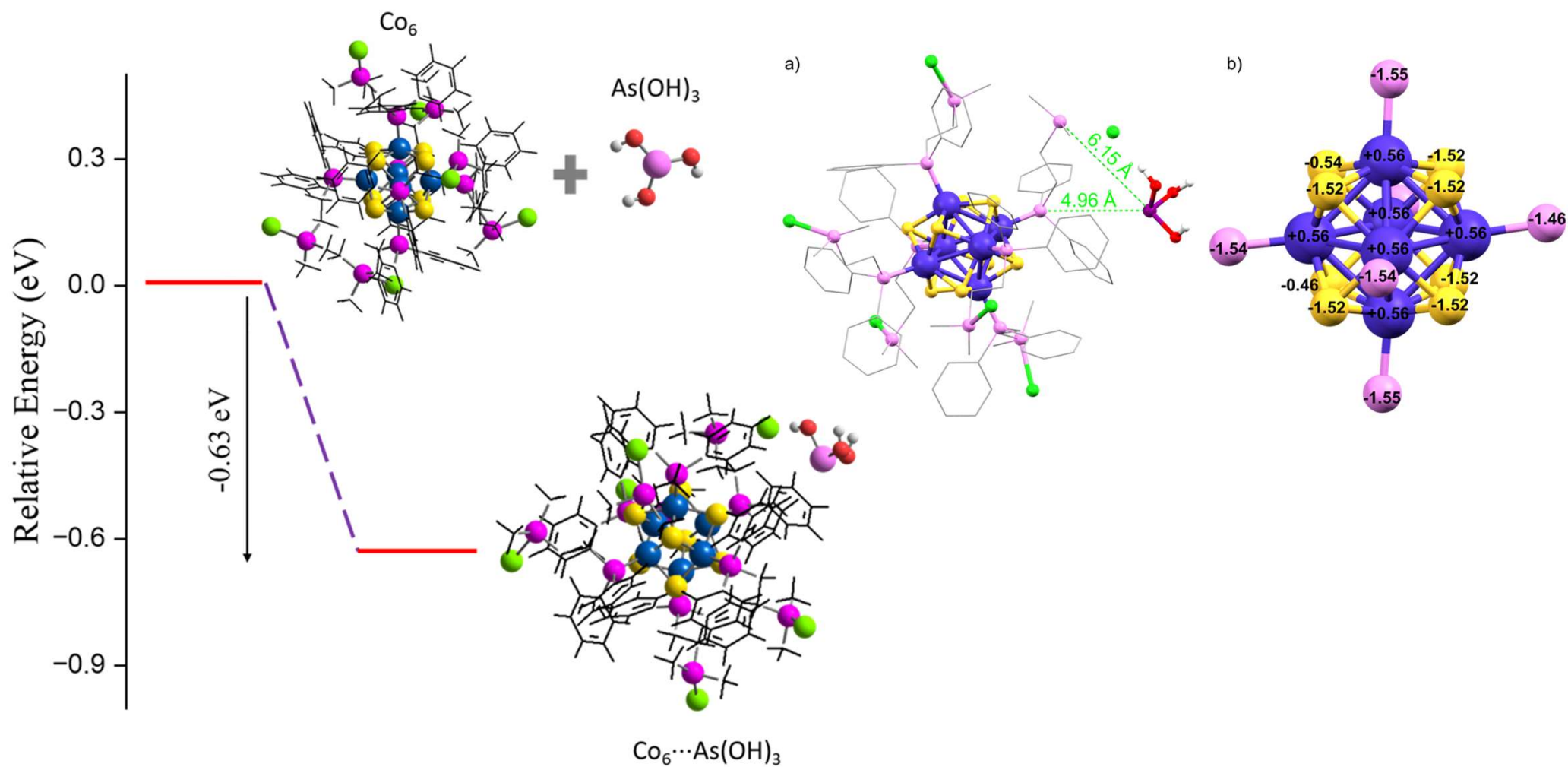
Electrospray deposition



Sensing



Computational insights



Previous As sensor with Co nanoparticles

1 μM = 75 ppb
10 μM = 750 ppb

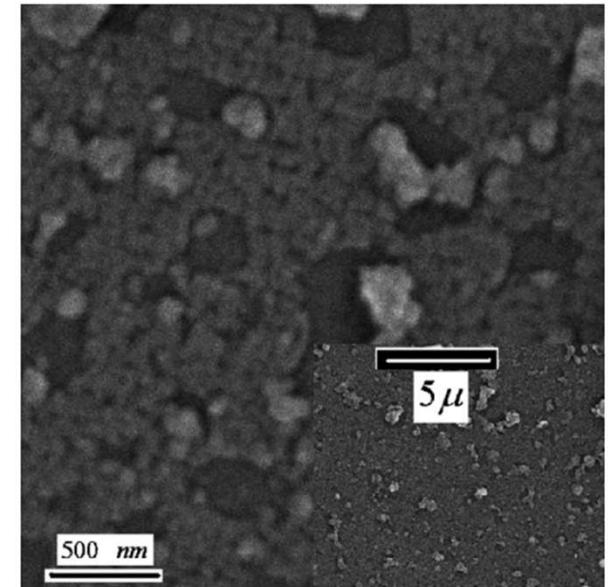
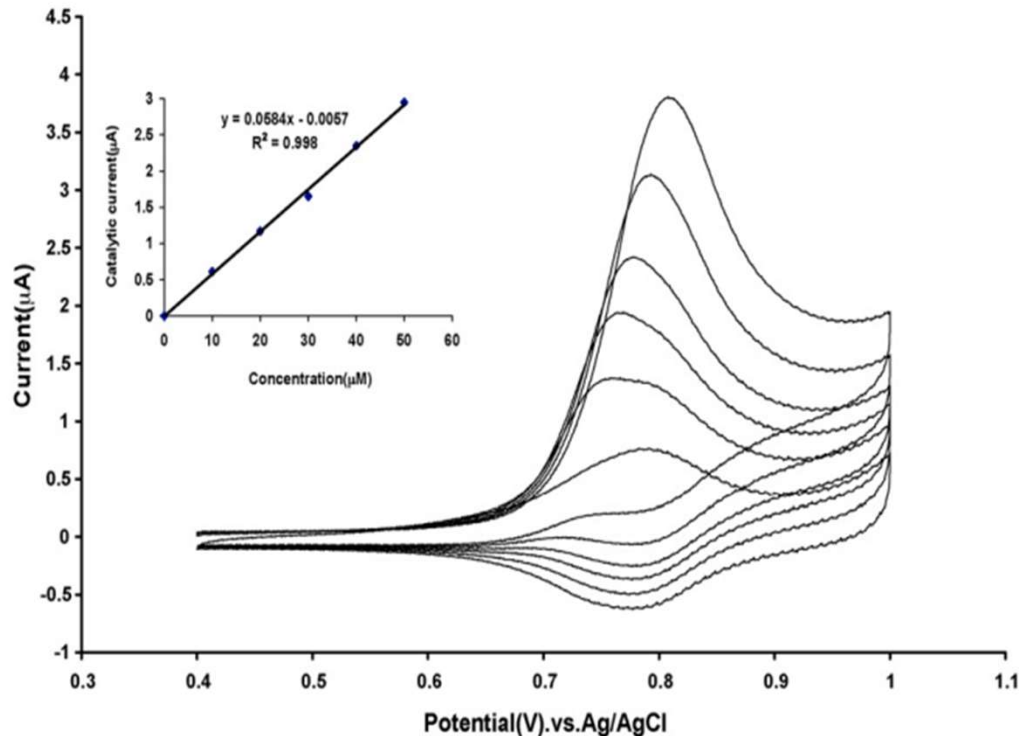
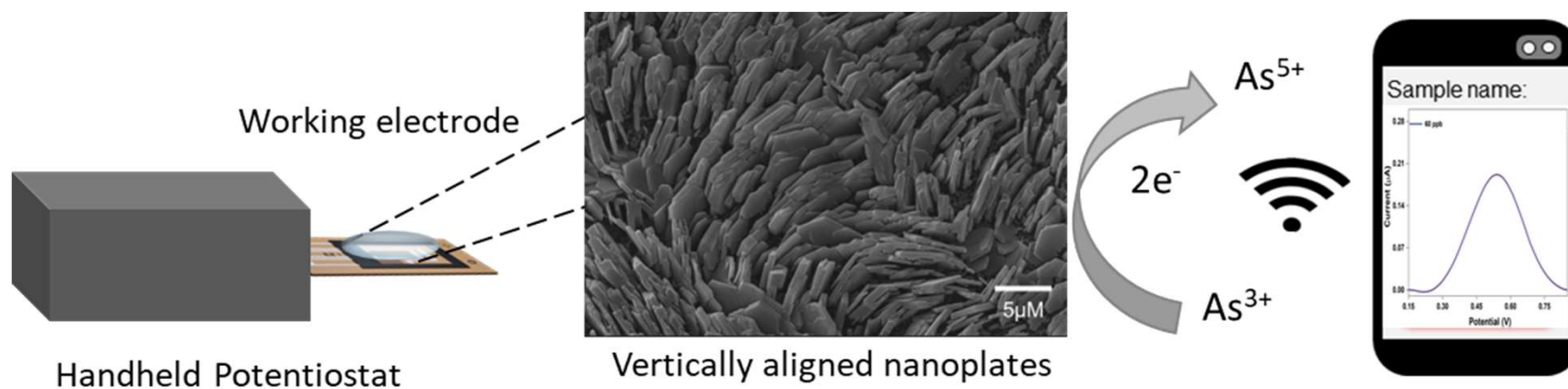
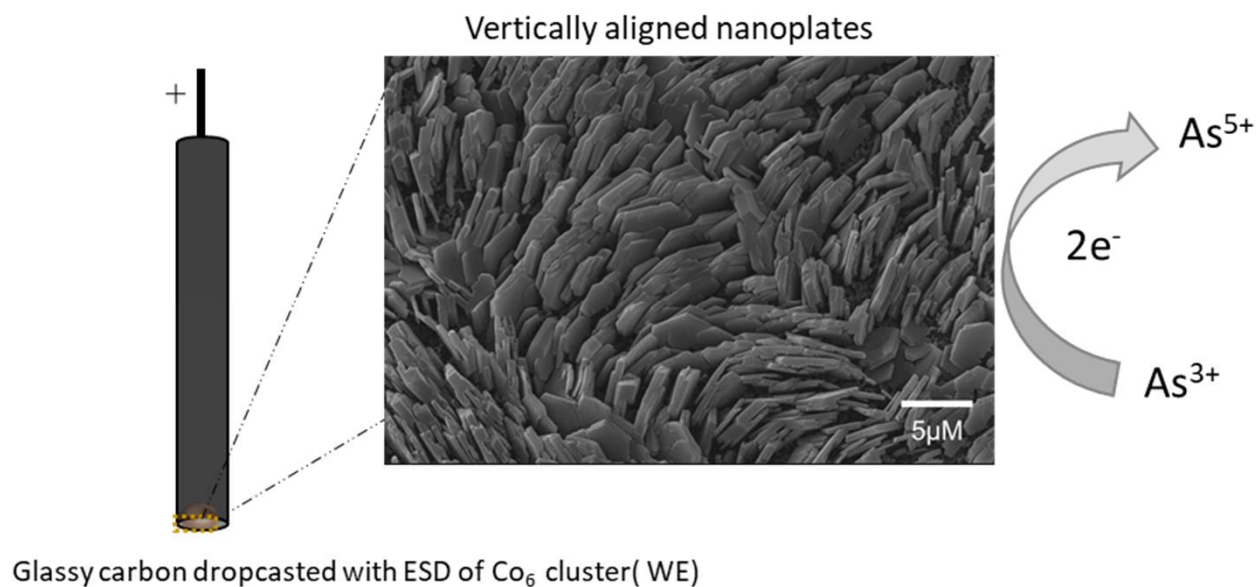


Fig. 1. SEM image of the electrodeposited cobalt oxide on glassy carbon, scale bar 500 nm. Inset: The SEM image with lower magnification for the same sample, scale bar is 5.0 μm .

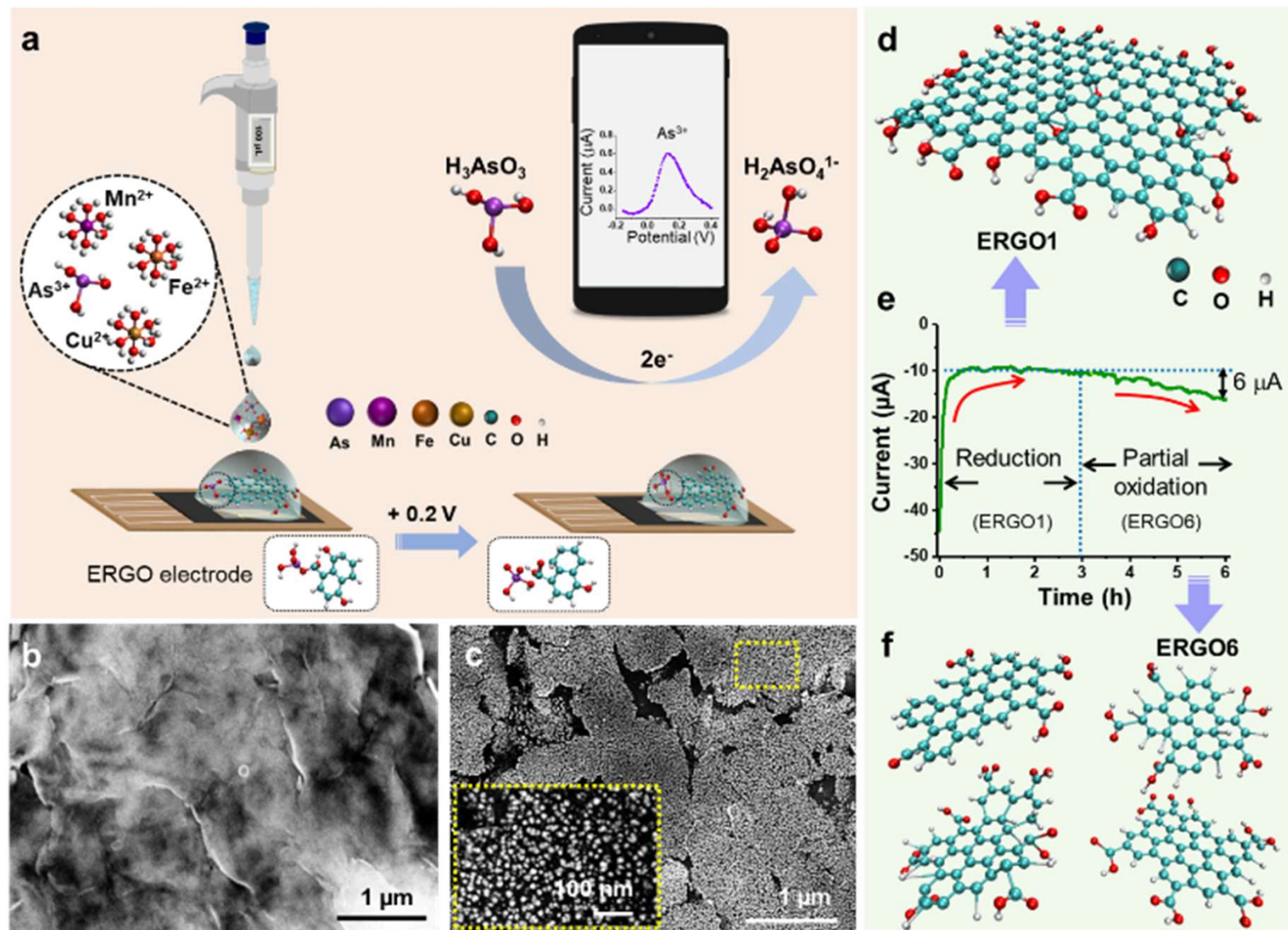
Fig. 4. Cyclic voltammograms of cobalt oxide nanoparticles modified GC electrode in buffer solution pH 7 at scan rate 20 mV s^{-1} with increasing arsenic concentration (from inner to outer) 0.0, 10, 20, 30, 40 and 50 μM . Inset: plot of peak current vs. arsenic concentrations.

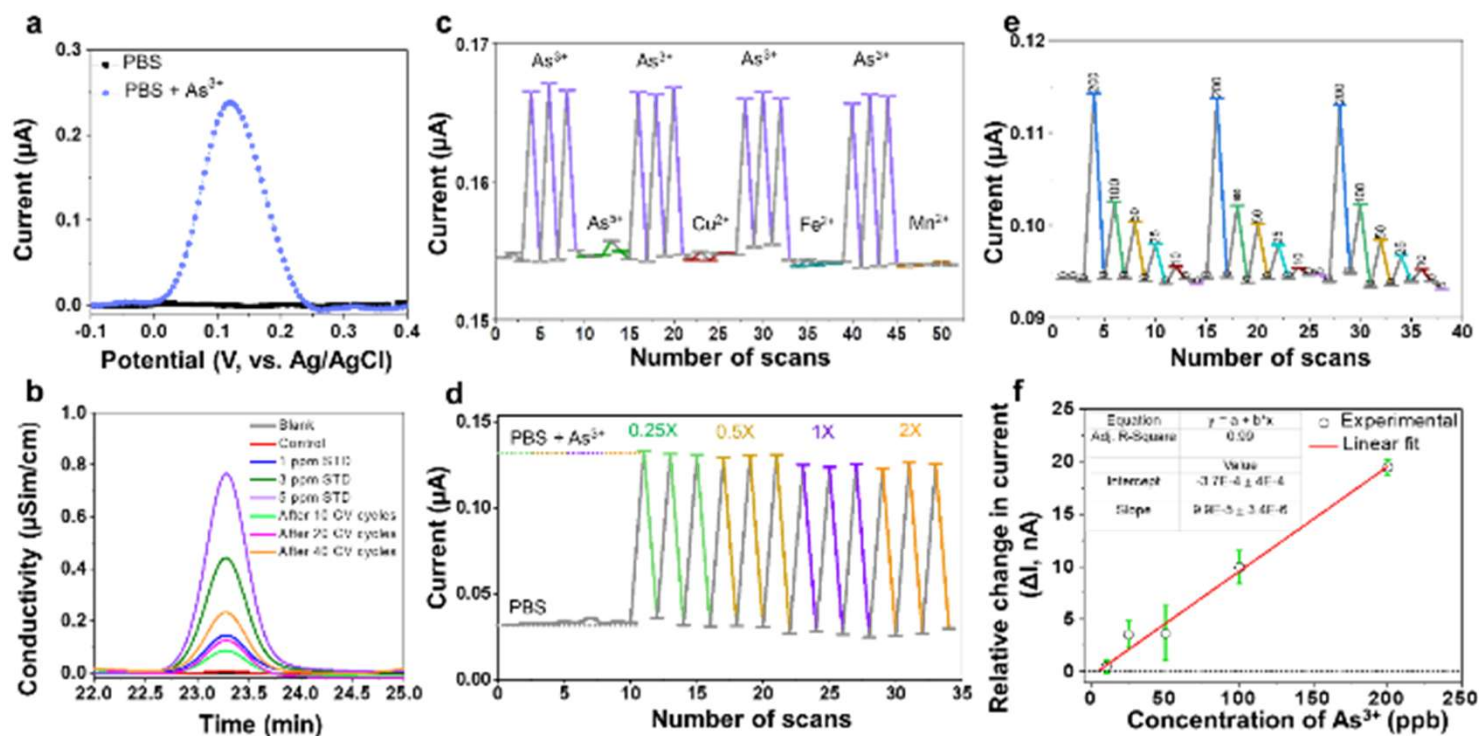
A theoretical LOD of 0.825 ppb using CoOx on a glassy carbon electrode in PBS at pH 7 was reported.

Working electrode

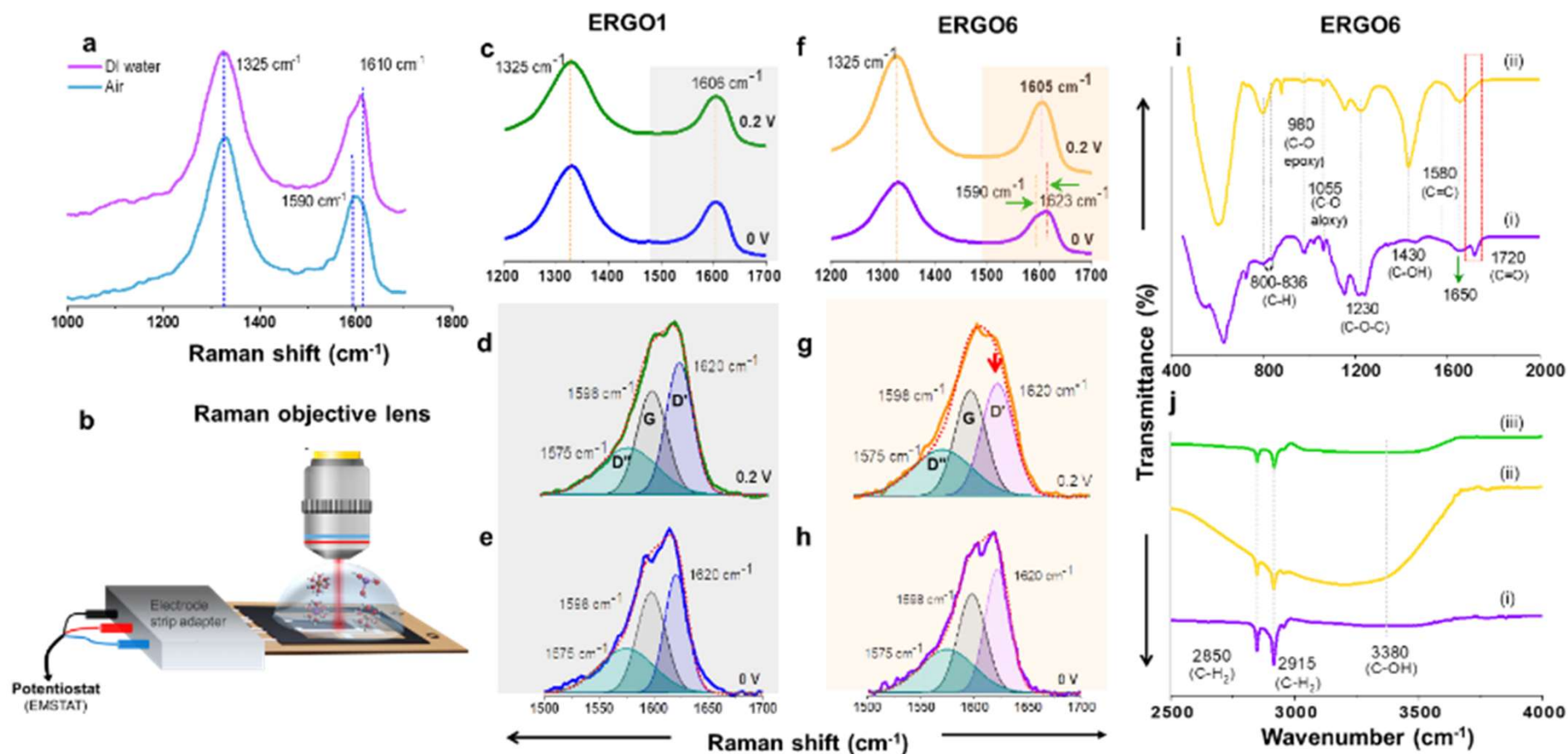


Practical graphene-based arsenite sensor



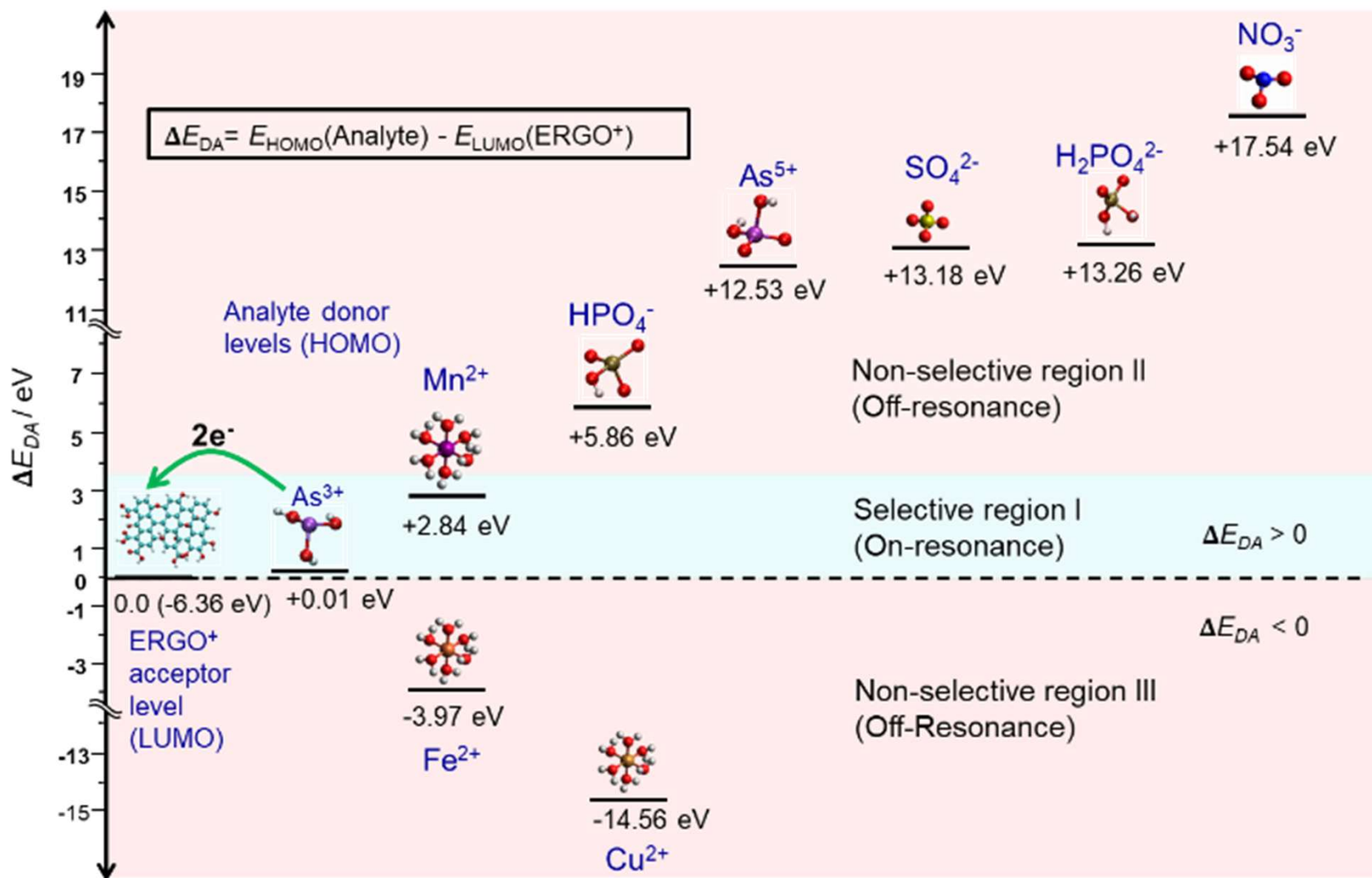


(a) LSV response of ERGO6 without and with 1 ppm As^{3+} , (b) Chronograms obtained from ion chromatography (IC) measurement with the solutions obtained after different number of CV cycles and same measurement with standard (STD) As^{5+} solutions of different concentrations. (c) CA measurement with different concentrations of As^{3+} . (d) Calibration curve showing linearity down to 10 ppb. (e) Interference study performed with several heavy metal ions with ERGO6 electrode. Concentration of As^{3+} was fixed at 200 ppb, while 1 ppm was maintained for interfering ions. (f) Investigation of CA current response of 1 ppm As^{3+} spiked in PBS with different ionic conductivity. We prepared PBS solutions of different conductivity by changing their ionic concentrations and used them further as electrolytes during CA measurements.

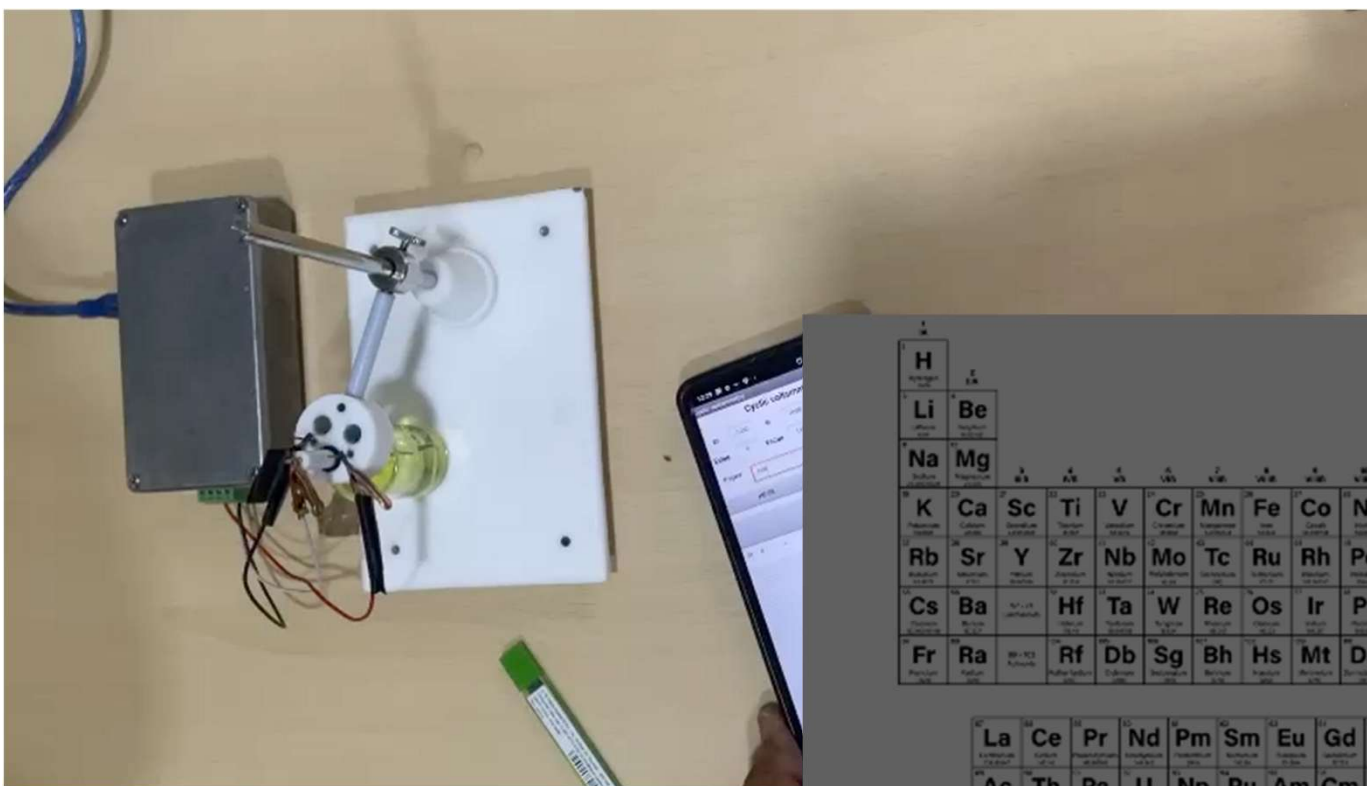


(a) Raman spectra of ERGO6 without (air) and with DI water. (b) Schematic depicts spectro-electrochemical (SPECT) measurement set-up. During SPECT measurements, the Raman objective was focused at the surface of ERGO6 strips with and without As^{3+} containing DI water on it and a DC potential of 0.2 V was applied to the electrode. (c) Raman spectra of ERGO1 in presence of As^{3+} without and with the application of potential (+ 0.2 V). Gaussian peak fitting was performed on the G bands of Raman spectra of ERGO1 (d) with, and (e) without the application of potential. (f) Raman spectra of ERGO6 in presence of As^{3+} without and with application of +0.2 V. Gaussian peak fitting was performed on the G bands of the Raman spectra of ERGO6 (g) with and (h) without the application of potential. Decrease in the intensity of D' is marked with a downward arrow. FTIR spectra of ERGO6 (i) without (purple trace) and with As^{3+} (yellow trace), (j) FTIR spectra of the same strip without As^{3+} (purple trace), with As^{3+} (yellow trace), and after electrochemical oxidation (green trace) to show the changes in OH deformation peak at higher wavenumber.

Origin of selectivity



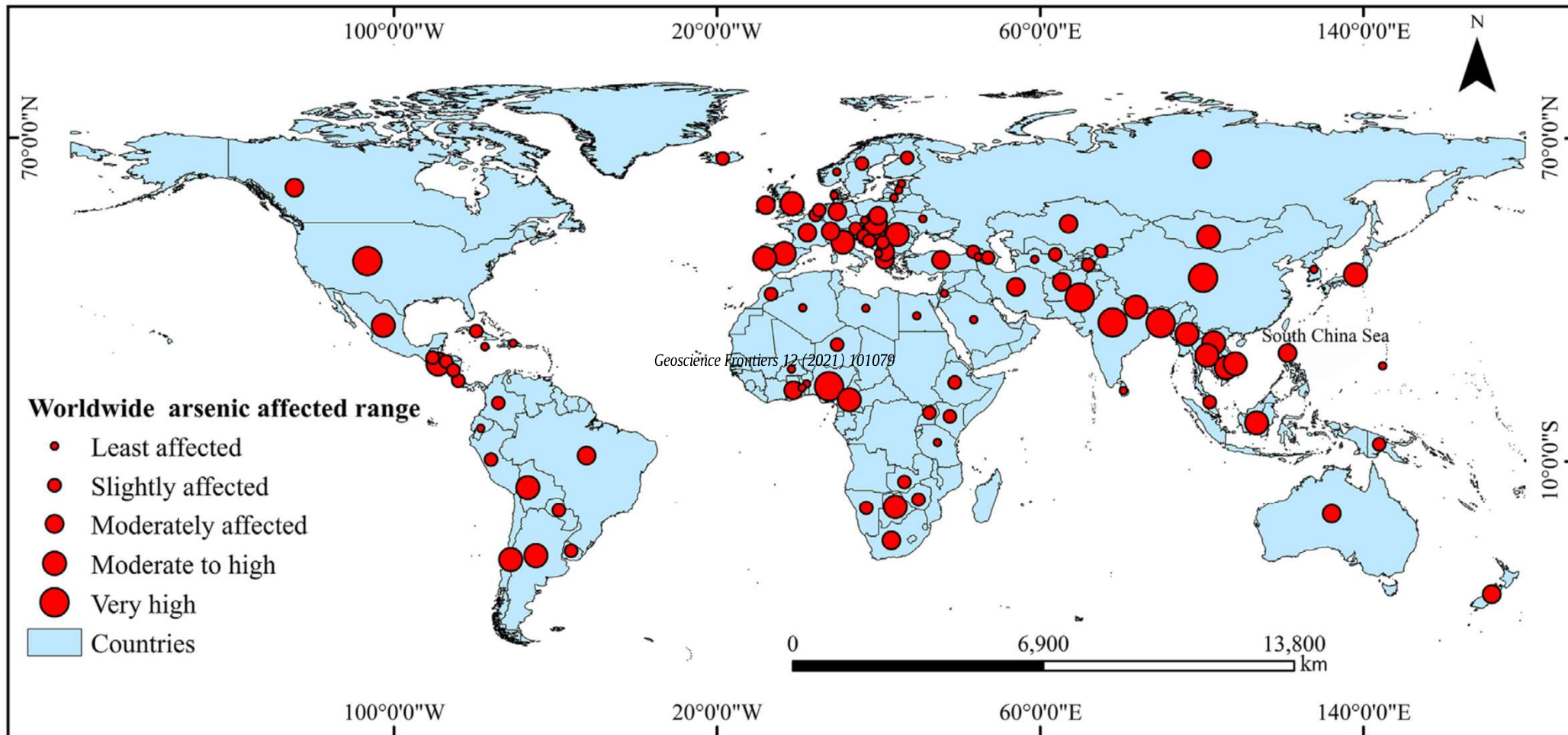
Analytical devices



1	2											10							
H	He											He							
3	4											5	6	7	8	9	10	11	12
Li	Be											B	C	N	O	F	Ne		
11	12											13	14	15	16	17	18		
Na	Mg											Al	Si	P	S	Cl	Ar		
19	20	21	22	23	24	25	26	27	28	29	30	31	32	33	34	35	36		
K	Ca	Sc	Ti	V	Cr	Mn	Fe	Co	Ni	Cu	Zn	Ga	Ge	As	Se	Br	Kr		
37	38	39	40	41	42	43	44	45	46	47	48	49	50	51	52	53	54		
Rb	Sr	Y	Zr	Nb	Mo	Tc	Ru	Rh	Pd	Ag	Cd	In	Sn	Sb	Te	I	Xe		
55	56	57	58	59	60	61	62	63	64	65	66	67	68	69	70	71	72		
Cs	Ba	Hf	Ta	W	Re	Os	Ir	Pt	Au	Hg	Tl	Pb	Bi	Po	At	Rn			
87	88	89	90	91	92	93	94	95	96	97	98	99	100	101	102	103	104		
Fr	Ra	Rf	Db	Sg	Bh	Hs	Mt	Ds	Rg	Cn	Nh	Fl	Mc	Lv	Ts	Og			
		89	90	91	92	93	94	95	96	97	98	99	100	101	102	103	104		
		La	Ce	Pr	Nd	Pm	Sm	Eu	Gd	Tb	Dy	Ho	Er	Tm	Yb	Lu			
		Ac	Th	Pa	U	Np	Pu	Am	Cm	Bk	Cf	Es	Fm	Md	No	Lr			

Sourav Kanti Jana

Arsenic poisoning across the world



Collaborators



Robin Ras

Nonappa

Tomas Base



Manfred Kappes

Olli Ikkala

Horst Hahn

Tatsuya Tsukuda,
Keisaku Kimura,
Yuichi Negishi,
Uzi Landman,
Hannu Hakkinen,
Rob Whetten



Shiv Khanna

Biswarup Pathak K. V. Adarsh

G. U. Kulkarni

Vivek Polshettiwar





Department of Science and Technology

Collaborators: Tatsuya Tsukuda, Keisaku Kimura, Yuichi Negishi, Uzi Landman, Rob Whetten, Hannu Hakkinen, Robin Ras, Manfred Kappes, Horst Hahn, Tomas Base, Nonappa, Shiv Khanna, Umesh Waghmare, Chandrabhas Narayana, Giridhar U. Kulkarni, Reji Philip, Vivek Polshettiwar, R. Mukhopadhyay, K. V. Adarsh, Biswarup Pathak, Chaitanya Sharma Yamijala

Thank you all